

Review

# A Comprehensive Overview of Recycled Glass as Mineral Admixture for Circular UHPC Solutions

N. Marcela Redondo-Pérez <sup>1</sup>, Jesús D. Redondo-Mosquera <sup>2</sup> and Joaquín Abellán-García <sup>1,\*</sup>

<sup>1</sup> Department of Civil and Environmental Engineering, Universidad Del Norte, Barranquilla 081007, Colombia; nrurys@uninorte.edu.co

<sup>2</sup> Department of Civil Engineering, Universidad de La Guajira, Riohacha 440002, Colombia; jesusdredondo@uniguajira.edu.co

\* Correspondence: jabellan@uninorte.edu.co

**Abstract:** This review article analyzes the influence of recycled glass (as sand and powder) beyond the durability, rheology and compressive strength of plain UHPC, even exploring flexural and direct tensile performance in fiber-reinforced UHPC. Interactions with other mineral admixtures like limestone powder, rice husk ash, fly ash, FC3R, metakaolin and slags, among others, are analyzed. Synergy with limestone powder improves rheology, reducing superplasticizer usage. Research highlights waste glass–UHPC mixtures with reduced silica fume and cement content by over 50% and nearly 30%, respectively, with compressive strengths exceeding 150 MPa, cutting costs and carbon footprints. Furthermore, with the proper fiber dosage, waste glass–UHPC reported values for strain and energy absorption capacity, albeit lower than those of traditional UHPC formulations with high cement, silica fume and quartz powder content, surpassing requirements for demanding applications such as seismic reinforcement of structures. Moreover, durability remains comparable to that of traditional UHPC. In addition, the reported life cycle analysis found that the utilization of glass powder in UHPC allows a greater reduction of embedded CO<sub>2</sub> than other mineral additions in UHPC without jeopardizing its properties. In general, the review study presented herein underscores recycled glass's potential in UHPC, offering economic and performance advantages in sustainable construction.



**Citation:** Redondo-Pérez, N.M.; Redondo-Mosquera, J.D.; Abellán-García, J. A Comprehensive Overview of Recycled Glass as Mineral Admixture for Circular UHPC Solutions. *Sustainability* **2024**, *16*, 5077. <https://doi.org/10.3390/su16125077>

Academic Editors: Anibal C. Maury-Ramirez and Nele De Belie

Received: 13 May 2024  
Revised: 7 June 2024  
Accepted: 12 June 2024  
Published: 14 June 2024



**Copyright:** © 2024 by the authors. Licensee MDPI, Basel, Switzerland. This article is an open access article distributed under the terms and conditions of the Creative Commons Attribution (CC BY) license (<https://creativecommons.org/licenses/by/4.0/>).

**Keywords:** waste glass; ultra-high-performance concrete (UHPC); life cycle analysis; circular economy; mineral admixtures; compressive strength; rheology; durability; post-cracking behavior; sustainability

## 1. Introduction

Over the past few years, notable advancements in concrete technology have occurred, leading to the creation of innovative concretes, like ultra-high-performance concrete (UHPC) [1,2]. With water-to-binder ratios (w/b) ranging from 0.15 to 0.25, UHPC showcases exceptional mechanical and durability properties that outperform standard concrete (SC) and high-performance concrete (HPC) [3,4]. According to the ACI-239 guidelines [5], UHPC features compressive strengths (CS) of over 150 MPa, along with an elastic modulus (MoE) within the range of 40 to 50 GPa. In addition, UHPC has exceptional durability features, which marks it as a promising construction material [6,7]. Despite its inherent brittleness, the practice of incorporating fibers, which has become widespread, successfully provides ductility and toughness to UHPC [8–13].

As observed in previous studies, a typical UHPC formulation encompasses Portland cement, reactive powders (such as silica fume (SF)), polycarboxylate-based superplasticizers, water and fine quartz sand (QS) [3,14,15]. Balancing the arrangement of the constituents is crucial to achieving this specialized cementitious material's outstanding mechanical and durability characteristics [16–18]. For instance, it is important to note that UHPC mixture design greatly depends on particle-packing theories to attain the optimal arrangement of particles [9,19]. The latter is key to achieving a microstructure that exceeds that of typical or even high-performance concrete [14,20].

For a thorough analysis of the unique properties displayed by UHPC, it is essential to consider three crucial factors: (a) the cementitious matrix reinforcement, (b) the porosity reduction and (c) the interfacial transition zone (ITZ) narrowing and densification [1,21,22]. Therefore, the approach of new UHPC formulations, such as those that incorporate recycled glass, must be carried out with care not to harm these three balances previously considered. Moreover, it is important to notice that with a reduced  $w/b$ , the cement hydration in UHPC is restricted, resulting in only partial calcium silicate hydrate (C-S-H) and calcium hydroxide (CH) formation [12,14,21]. By utilizing highly reactive pozzolanic mineral admixtures, like SF, the hydrated cement paste can be strengthened through the formation of secondary C-S-H by its reaction with CH [21]. Therefore, it is essential to find the perfect equilibrium between cement quality and content and pozzolanic materials in UHPC to effectively enhance its strength [1]. One important aspect is to decrease the porosity of the concrete by using a low  $w/b$  and achieving an enhanced packing density [23]. This way, one must meticulously choose micro- and nano-sized components that can effectively fill the gaps between larger particles, resulting in an improved packing arrangement [22]. It is worth mentioning that certain materials, like SF, quartz powder, slags, fly ash and others, are frequently utilized in this application owing to their fine particle size and pozzolanic features [2,3,6,23–29]. Understanding the achievement of optimal density in concrete relies on the use of particle-packing models, like the modified Andreasen and Andersen (A&Amod) or the Compressive Packing Model (CPM) [19]. The optimal packing density plays a crucial role in lessening interparticle gaps, constraining the space for portlandite crystal growth. In order to obtain the requisite low porosity in UHPC, it is essential to include superplasticizers, which help reduce the  $w/b$  to a minimum [20,30]. Due to its unique properties, UHPC has a lower porosity of approximately half of that of the average porosity found in standard concrete [5]. Furthermore, enhancing the strengthening properties of the UHPC matrix can be accomplished by decreasing the maximum aggregate size, encouraging compact particle arrangement and utilizing a low  $w/b$ . This improves the ITZ that separates the bulk paste and aggregate [14]. However, the removal of coarse aggregates results in a higher amount of powders, such as cement and SF, being needed. This can have negative effects on cost and sustainability, as will be explored in later sections [25,28].

With its exceptional properties, UHPC proves to be incredibly beneficial in a broad variety of structural and infrastructure uses. The exceptional mechanical properties of this special concrete can be leveraged to create structures with reduced weights by designing reduced cross-sectional areas. Moreover, the exceptional durability of the material extends its lifespan and minimizes the requirement for maintenance, resulting in decreased expenses [21]. Therefore, UHPC is widely used in different areas of the construction industry, such as footbridge construction, retrofitting of existing structures, pavement restoration, tunnel boring machine segments, the ABC bridge construction system, facades and urban furniture [4,12,31–38]. These examples of various applications demonstrate the flexibility and potential of UHPC in addressing the changing requirements of contemporary construction projects.

However, as previously stated, UHPC production requires large amounts of cement, SF and quartz powder, leading to higher costs and a greater impact on the environment [23]. As a result, these limitations have impeded an even more widespread utilization of UHPC around the world [23]. The global research community has been diligently working on addressing this challenge by investigating the potential of alternative components for making UHPC. These components can be employed as cement and SF partial replacements in new formulations. Hence, through extensive research and analysis, most scholars strive to minimize expenses and improve the material life cycle, narrowing the knowledge gap and exploring new avenues for creating UHPC mixtures that are both sustainable and economically viable [12,24,34,39].

For its part, the utilization of glass powder (GP) in UHPC has garnered considerable attention in recent years, yielding substantial advancements in both understanding its

properties and practical implementation in construction [40–42]. As a substitute for traditional fillers and pozzolanic materials, glass powder offers unique advantages within concrete mixes [43,44]. Concurrently, the proliferation of waste glass (WG) worldwide has escalated dramatically, resulting in significant environmental pollution [44–46]. This surge in WG underscores the urgent need for sustainable solutions. Furthermore, rising costs and carbon emissions associated with conventional high-strength concrete production have underscored the demand for alternative supplementary cementitious materials [26,47,48].

Chemically, glass comprises inorganic compounds fused at high temperatures and cooled to a solid state, typically consisting of calcium oxide, sodic oxide and non-crystalline silica, though composition varies based on application [40,49–51]. Historically, waste glass has found utility in hydraulic concrete production as a supplementary cementitious material and fine aggregate, owing to its high silica content. Effective recycling strategies are pivotal in preserving the purity and quality of glass [40,49–51]. In this context, GP, obtained by milling WG, emerges as a promising candidate for partially replacing cement in alternative UHPC formulations, leveraging its pozzolanic properties to enhance mechanical characteristics while allowing for substantial cement, silica fume or quartz powder reductions [51–53]. However, careful attention must be directed towards mitigating the potential alkali-silica reaction (ASR) risk introduced by GP particles [54].

This convergence of research underscores the potential of GP as an environmentally friendly solution in UHPC formulations, offering both environmental benefits and economic viability in the construction sector. This review is the first to provide a global perspective, spanning from microstructure to real-world applications. It covers the most relevant mechanical properties, such as the direct tensile behavior of recycled-glass UHPC reinforced with fibers, and examines the effects on costs and carbon footprint. Additionally, it presents a comprehensive overview of UHPC properties containing waste glass in both fresh and hardened states, while also analyzing the advantages, opportunities and risks of using such supplementary cementitious waste material in UHPC formulations. Figure 1 puts forward a scheme of the structure of the review study presented herein.

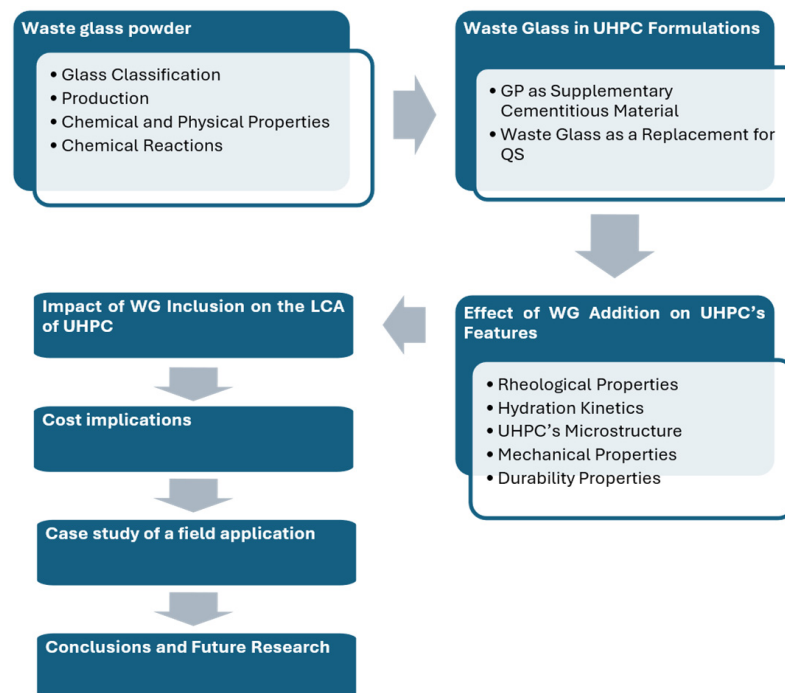


**Figure 1.** Structure of the review study presented herein.

## 2. Research Significance

In recent years, there has been a concerted scholarly effort focused on harnessing the potential of GP as a substitute for conventional UHPC-making materials [1,47,55–59].

This approach is driven by the need to address stringent environmental impacts and the escalating costs associated with typical UHPC mixtures, due to their high amount of expensive and/or high carbon footprint raw constituents, like SF, cement or QP. On the one hand, it is imperative to recognize that all materials, including glass, have a finite lifespan and must be recycled or repurposed to mitigate environmental risks [44,60]. Therefore, by incorporating waste glass into concrete production, even UHPC, researchers aim to minimize solid waste, maximize recycling efforts, conserve natural resources and mitigate environmental hazards associated with landfilling [41,44,60]. On the other hand, the employment of WG in concrete offers multifaceted benefits, encompassing the reduction of landfill tipping fees, which typically range from \$40 to \$100 per ton in the USA [61]. Moreover, the integration of WG as a replacement for typical UHPC-making components in alternative formulations can significantly lower material costs, enhance sustainability and reduce environmental impacts [24,62]. Particularly, by replacing quartz powder, cement and even silica fume with ground glass powder, substantial cost reductions can be achieved in traditional UHPC [63,64]. Waste glass presents a notably lower cost compared to quartz powder, with a price approximately one-third less expensive. Moreover, the utilization of locally sourced waste glass for UHPC production contributes to decreased transportation expenses for materials [41], and also reduces glass waste disposal and, therefore, its associated costs [44]. Furthermore, WG incorporation into concrete production helps reduce CO<sub>2</sub> emissions, energy consumption and air pollution associated with conventional cement clinker production [61]. In addition, incorporating glass powder in UHPC formulations eliminates the need for quartz powder, a known carcinogen, thereby enhancing the safety of the UHPC production process [1,52]. Hence, the strategy of using recycled glass in UHPC production aligns with the broader goal of promoting environmental stewardship and fostering a more sustainable and safer construction industry.

Hence, this review article's purpose is to offer a thorough analysis of the technical, economic and environmental implications, as well as the limitations and possible risks surrounding incorporating recycled waste glass in UHPC production. To that end, the findings of a total of 157 research papers, dissertation theses and proceedings articles including information about rheological, mechanical and durability characteristics, besides costs and carbon footprint implications, were analyzed, organized and presented.

### 3. Waste Glass Powder

#### 3.1. Glass Classification

This section offers a succinct overview of the primary classifications of waste glass, examining two classification methods while providing detailed insights into their chemical composition and application. On the one hand, concerning chemical composition, WG may be categorized into four main classes: soda-lime glass, lead glass, borosilicate glass and electric glass, also known as E glass [65]. Soda-lime glass finds widespread application in various glass products, including containers and plates. Hence, more than 90% of the glass produced in the European Union corresponds to this type of glass [65]. Even though the chemical compositions across different glass types primarily comprise silica (SiO<sub>2</sub>), sodium oxide (Na<sub>2</sub>O) (derived from soda ash (Na<sub>2</sub>CO<sub>3</sub>)) and lime (CaCO<sub>3</sub>), among others, there are some differences in their proportions [66]. On the other hand, in terms of application, glass can be broadly classified into several categories, each serving distinct purposes. These categories encompass container glass, plate glass (e.g., window glass), continuous filament glass (including roving, mat, textile and optical fiber), domestic glass or tableware, insulation mineral wool and specialty glass (such as high-temperature domestic glass). Each type of glass corresponds to specific applications; for instance, soda-lime glass and plate glass are commonly employed in container and window manufacturing, respectively. Continuous filament glass predominantly consists of electric glass, while domestic glass can vary between soda-lime glass and lead glass. Insulation mineral wool is derived from borosilicate glass, whereas specialty glass typically comprises soda-lime glass

or borosilicate glass [65,67]. Table 1 provides a comprehensive breakdown of the chemical compositions associated with various types of glass [67].

**Table 1.** Major components of the different classes of glass regarding their chemical composition [67].

	Soda-Lime	Lead	Borosilicate	E-Glass
SiO <sub>2</sub>	71–75%	54–65%	70–80%	52–56%
Al <sub>2</sub> O <sub>3</sub>	1–1.5%		7%	12–16%
B <sub>2</sub> O <sub>3</sub>			7–15%	0–10%
CaO	9–15%			16–25%
PbO		25–30%		
Na <sub>2</sub> O+	12–16%	13–15%	4–8%	0–2%
K <sub>2</sub> O				

Moreover, glass can be categorized into three types based on color: (i) clear/flint glass, (ii) green glass and (iii) brown/amber glass. These color variations are attributed to distinct chemical compositions, each with specific thresholds for color impurities. The acceptable range for color contamination is 4–6% for clear glass, 5–30% for green glass and 5–15% for amber glass [65]. When it comes to glass aggregate, green glass exhibits superior resistance to ASR reaction due to its high concentration of Cr<sub>2</sub>O<sub>3</sub>, which effectively mitigates ASR growth [68]. However, due to the particularities of UHPC, other factors such as the particle glass size and the presence and dosage of high pozzolanic supplementary cementitious materials such as SF play more crucial roles in determining ASR formation [50,68,69]. The chemical compositions of different colored glasses are detailed in Table 2 [65].

**Table 2.** Different color glass chemical compositions reported in the scientific literature [65].

	Glass Color		
	Green	Brown/Amber	Clear/Flint
SiO <sub>2</sub>	71.3%	71.9–72.4%	73.2–73.5%
Al <sub>2</sub> O <sub>3</sub>	2.20%	1.70–1.80%	1.7–1.9%
SO <sub>3</sub>	0.05	0.12–0.14%	0.20–0.24%
CaO + MgO	12.20%	11.60%	10.7–10.8%
Fe <sub>2</sub> O <sub>3</sub>	0.56%	0.30%	0.04–0.05%
Na <sub>2</sub> O + K <sub>2</sub> O	13.10%	13.8–14.4%	13.6–14.1%
Cr <sub>2</sub> O <sub>3</sub>	0.43%	0.01%	-

### 3.2. Production

WG is found in municipal solid waste (MSW) as containers, cullets and plate residues. While the majority of the data focus on glass containers, several evaluations also include glass components used in long-lasting items including furniture, appliances and consumer electronics. In 2018, the United States and Europe consumed 12.25 and 16.36 million tons of glass and recycled 3.1 and 12.92 million tons, respectively, for a recycling rate of 31.3% in the case of the USA and 76% in Europe [70,71]. For this part, China generated approximately 20 million tons of glass waste in the same year, with 53% being recycled [72]. In the case of Australia, about 1.1 million tons of WG were produced in 2018, with the recycling rate in the range between 54 and 61% [73]. In contrast, Sweden has achieved a remarkable glass recycling rate exceeding 90% for the same period of time, ranking among the highest in the world [74].

### 3.3. Chemical and Physical Properties

Table 3 depicts the chemical characterization of the glass in different studies about its use in UHPC formulations carried out previously. As all of the below are soda-lime class, it

is observed that the percentages have values close to each other. In other words, although they are different glass powders, their chemical composition is similar. Some interesting findings observed in Table 3 are the high amount of silica oxide (over 79% in all cases) and the alkali content (in the range of 12.4–13.5%). These values have a relevant impact on the concrete's properties and potential damages, as will be seen in future sections of this document.

**Table 3.** Chemical composition of glass powder reported in UHPC research.

Components	Glass Powder References					
	[29]	[75]	[76]	[77]	[48]	[64]
SiO <sub>2</sub>	72.89	75.47	72.2	73.00	71.4	72.76
Al <sub>2</sub> O <sub>3</sub>	1.67	1.09	1.54	1.5	1.4	1.67
Fe <sub>2</sub> O <sub>3</sub>	0.81	0.79	0.48	0.4	0.2	0.79
CaO	9.73	9.02	11.42	11.3	10.6	9.74
MgO	2.08	1.97	0.79	1.2	2.5	2.09
SO <sub>3</sub>	0.01	-	0.09	-	0.1	0.10
Na <sub>2</sub> O	12.54	11.65	12.85	13	12.7	12.56
K <sub>2</sub> O	0.76	0.75	0.43	0.5	0.5	0.76
TiO <sub>2</sub>	0.04	0.04	-	0.04	-	0.04

Figure 2 presents the X-ray diffraction (XRD) analysis conducted on WG particles utilized in UHPC research [12,49]. As can be observed, the reported XRD analysis of recycled glass particles reveal their amorphous nature, characterized by a minor presence of long-range atomic order. This amorphous phase, typical of soda-lime glass materials [47,49,50,59,78], is a key factor in their pozzolanic activity when used as glass powder in concrete [79,80]. The absence of crystalline structure allows for greater reactivity with calcium hydroxide during cement hydration, resulting in the creation of secondary C-S-H gel. This gel enhances the binding and strengthening properties of concrete, contributing to improved mechanical performance and durability [46,81]. Therefore, confirming the amorphous nature of recycled glass particles through XRD analysis is essential for evaluating their suitability as supplementary cementitious materials and predicting their effectiveness in enhancing concrete properties [50].

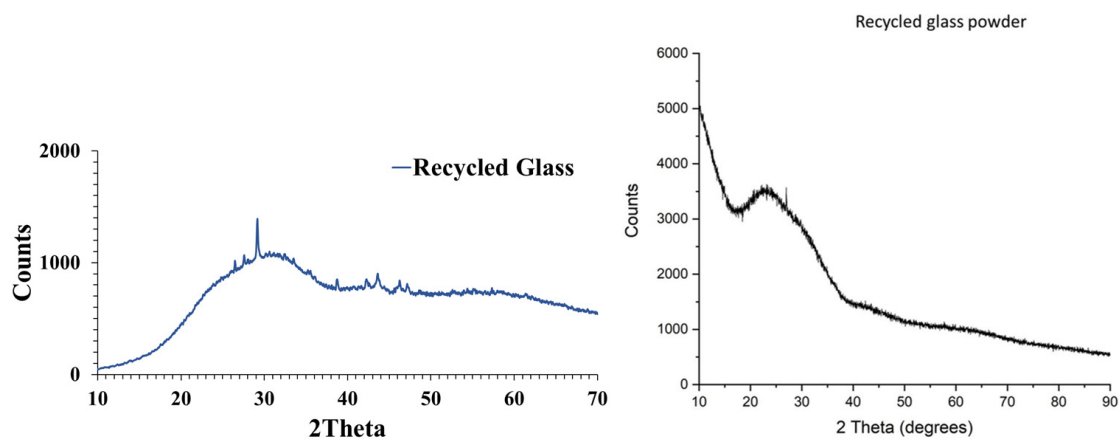


**Figure 2.** XRD analyses of milled waste glass used in UHCP formulations [12,49].

For its part, Table 4 presents some physical properties of recycled glass particles utilized in UHPC mixtures [24,42,59,64,75].

**Table 4.** Physical properties reported for milled waste glass particles utilized in UHPC [24,42,59,64,75].

Physical Feature	Value
Specific gravity	2.19–2.60
Water absorption (%)	0.19–0.4

Moreover, Figure 3 puts forward the SEM (Scanning Electron Microscopy) analysis of the particles of recycled waste glass utilized in several UHPC formulations [29,47,82,83]. As can be observed in Figure 3, these particles are characterized by their irregular shapes and angular edges, resulting from the mechanical grinding action applied during production. Their smooth surface and lack of porosity correlate well with the low water absorption depicted in Table 4.

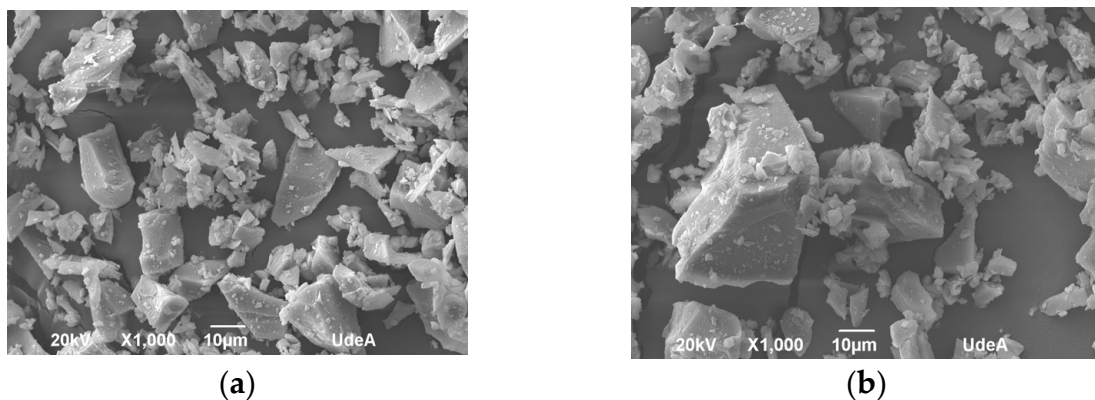
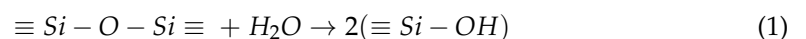


**Figure 3.** SEM analysis of milled waste glass used in UHPC formulations: (a) recycled glass powder ( $d_{50}$ : 7  $\mu\text{m}$ ) used as partial cement replacement [82], and (b) recycled glass flour ( $d_{50}$ : 28  $\mu\text{m}$ ) utilized as total QP replacement [29].

### 3.4. Chemical Reactions

Figure 4 illustrates the reactions of GP within concrete. Initially (Figure 4A), solid amorphous silica is depicted, followed by its dissolution in water (Figure 4B). The silica reactivity is contingent upon its amorphous silica rate and the pH of the pore solution, which dictates the dissolution rate. Equation (1) [84] describes this process.



When dissolved silica interacts with hydroxide ions  $\text{OH}^-$  in mixed concrete (see Figure 4C), three types of gel are produced, each contingent upon the environment. The first type is calcium silicate hydrate (Figure 4D), characterized by a pH range of 12–13 and an abundance of calcium ions ( $\text{Ca}^{2+}$ ). The second type is calcium aluminate silicate hydrate (Figure 4E), which shares a similar pH range of 12 or 13 and is rich in both calcium ions ( $\text{Ca}^{2+}$ ) and aluminum ions ( $\text{Al}^{3+}$ ). Lastly, alkali silica gel (Figure 4F) exhibits a higher pH exceeding 13 and is enriched with sodium ions ( $\text{Na}^+$ ) and potassium ions ( $\text{K}^+$ ) [84]. These three types of gel are expounded on in more detail in the next subsections.

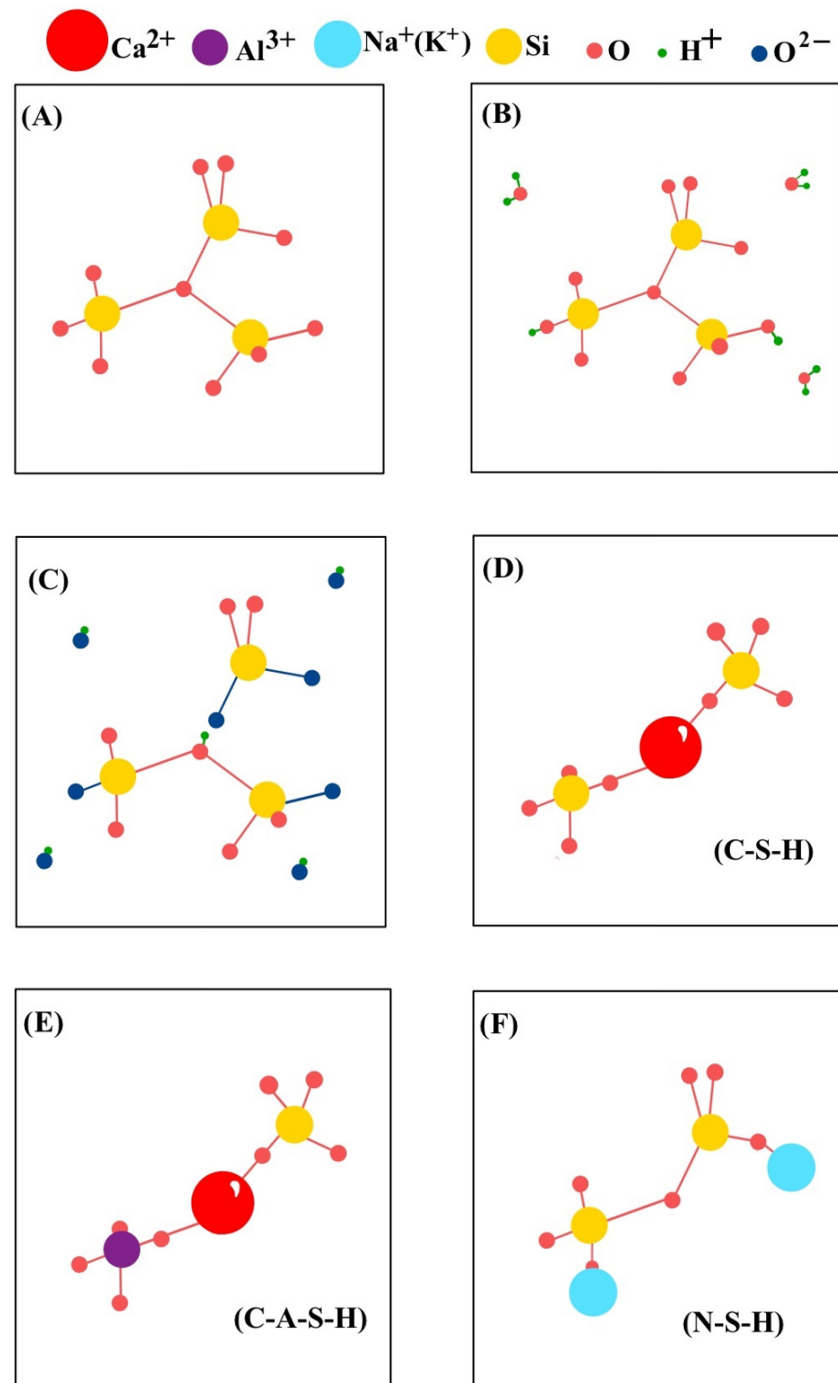


**Figure 4.** Glass reactions as a UHPC-making component [85]: (A) Solid amorphous silica; (B) Amorphous silica dissolution in water; (C) Dissolved silica interaction with hydroxide ions  $\text{OH}^-$ ; (D) Calcium silicate hydrate structure; (E) Calcium aluminate silicate hydrate structure; (F) Alkali silica gel structure.

### 3.4.1. Calcium Silicate Hydrate Gel

The main product of Portland cement hydration is C-S-H gel, which plays a crucial role in providing strength. This gel is characterized by its extensive and disordered atomic structure, contributing to the formation of a family of solubility curves within the  $\text{CaO} - \text{SiO}_2 - \text{H}_2\text{O}$  system. Structurally, most layers resemble tobermorite, while others exhibit imperfections akin to jennite. In addition to cement hydration, this gel can be produced by the pozzolanic reaction between CH and a material with amorphous silica, like GP, in the

presence of water [65,86]. Equation (2) [84] illustrates the pozzolanic reaction responsible for C-S-H production, where the coefficients  $x_1$  and  $x_2$  represent variable numbers [84].

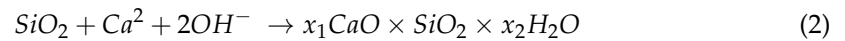


Figure 5 represents graphically that the pozzolanic reaction occurs when the  $\text{SiO}_2$  reacts with CH and creates C-S-H gel. Investigations showed that the pozzolanic reactivity of WG as a replacement for several percentages of the weight of cement (0, 15, 30, 40 and 60%), and this demonstrated that CS was not reduced by the substitution cement for WG. The pozzolanic reaction between waste glass or glass powder and cement hydration products allows the concrete not to lose strength. In the majority of replacement percentages, the compression resistance is 85% and allows for enhancements in durability owing to the refined microstructures of GP [51].

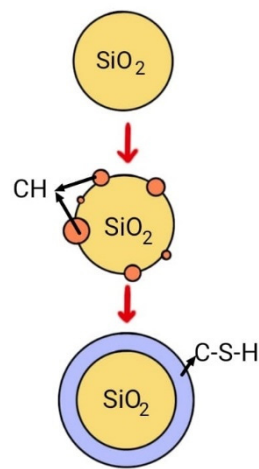
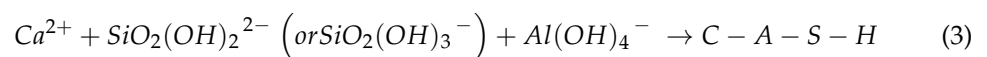


Figure 5. Pozzolanic reactions [85].

### 3.4.2. Calcium Aluminate Silicate Hydrate

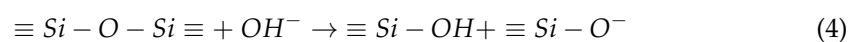
Calcium aluminate silicate hydrate (C-A-S-H) is a calcium silicate hydrate, but this is incorporating aluminum into its structure, as depicted in Figure 4A. Its usual atomic ratio of Al: Si is under 0.25. As can be seen in Figure 4E, the C-S-H adds an aluminum and this gel is shaped during Portland cement hydration in the presence of  $\text{Al}^{3+}$  ions [87].

To yield C-A-S-H gel the ions  $\text{OH}^-$  broke the bonds of Al-O and Si-O with a necessary high pH (between 12–13) to form  $\text{SiO}_2(\text{OH})_3^-$ ,  $\text{SiO}_2(\text{OH})_2^{2-}$  and  $\text{Al}(\text{OH})_4^-$ . Equation (3) [88] expresses the situation when the dissolved aluminate and silica react with  $\text{OH}^-$  and  $\text{Ca}^{2+}$  to produce C-A-S-H gel.

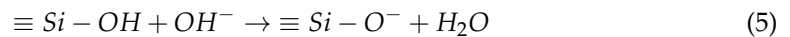


### 3.4.3. Alkali Silica Gel

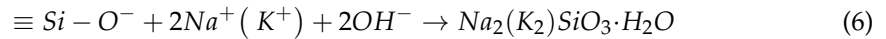
The third and last gel, the alkali-silica gel, is the one that is formed during the ASR reaction [79,89,90]. The alkali-silica reaction is considered a concrete disease because it is one of the main risky chemical reactions that is generated between aggregates with some reactive silica content alkalis of the cement (sodium hydroxide and/or potassium sodium) in the concrete. This consists of the generation of an expansive gel that meets water and produces an increase in the matrix volume, which yields the concrete mass to crack and destroy itself. Equation (3) [84] describes how the silica amorphous network becomes more reactive due to high pH (greater than 13) causing the siloxane chemical bond to be broken with the presence of  $\text{OH}^-$  to form new ions [85].



Once crystalline silicates bonds are formed ( $\equiv Si - OH$ ) they can react with  $OH^-$  and produce new ions, as presneted in Equation (5) [85].



As shown in the Equation (5), the  $\equiv Si - O^-$  which in turn reacts with potassium ( $K^+$ ) and sodium ( $Na^+$ ) also, with  $OH^-$  to produce alkali silica gel (N-S-H).



To mitigate the risk of ASR, several factors need careful control, including the water-cement ratio, aggregate size, alkali solubility, type of cement, alkali content, utilization of supplementary cementitious materials and the presence of reactive aggregates [88]. In this regard, the employment of WG powder in concrete composition offers high amounts of amorphous silica (see Table 3 and Figure 2) as well as alkalis (Table 3). Thereby, special care should be taken when incorporating this waste into concrete formulations. However, recent investigations consider that the GP should pass a 325-mesh sieve because the particles smaller than 300 microns do not present a risk for alkali-silica reaction [91].

#### 4. The Use of Waste Glass Powder in UHPC Formulations

##### 4.1. GP as Supplementary Cementitious Material

Various pieces of research have been conducted to define the role of milled WG as a replacement for typical UHPC-making powdered materials like cement, silica fume or quartz powder [3,44,52,75,92]. Results have pointed out how various properties of glass powder, such as particle size, impact the characteristics of UHPC [75,77]. These studies have examined the effects of glass particle size from fine powder ( $d_{50}$ : 3.8  $\mu m$ ), powder ( $d_{50}$ : 7  $\mu m$ ) or flour ( $d_{50}$ : 28  $\mu m$ ) [75,77]. Depending on the particle size, these pieces of research have utilized this waste material for substituting (totally or partially) SF, cement and quartz powder [47,75]. As packaging density and particle-size distribution of components determine UHPC design, Soliman & Tagnit-Hamou [77] employed fine glass powder ( $d_{50}$ : 3.8  $\mu m$ ) to partially replace SF in UHPC formulations. The findings of their research showed that substituting 30% and 50% of SF with this fine GP may obtain compressive strengths of 235 and 220 MPa after 2 days of heat curing, in comparison with 204 MPa for the control UHPC formulation. Moreover, the study also depicted that when SF particles were replaced with nonabsorptive glass particles, the fresh UHPC rheology was enhanced [77].

For their part, Abellán et al. [75] achieved CS over 150 MPa with more than 50% of replacement percentages in traditional materials like cement and quartz powder (QP) with glass powder (GP) and glass flour (GF). Their findings revealed that specific combinations led to a reduction in cement content, identifying a mixture comprising 603 kg of cement and over 0.5 kg/m<sup>3</sup> of glass powder (GP) and glass fibers (GF) per kg of cement. This formulation achieved a CS of 152 MPa within 28 days under standard curing.

Tagnit-Hamou et al. [52] studied the implication of the curing temperature and the amount of water in CS of waste glass-UHPC at 2, 28 and 91 days. The tests pointed out that the inclusion of GP as a cement partial replacement increases the spread flow, a factor that allows it to work with a lower w/b [27,75]. Also, with more than 20% of cement replacement with GP, the CS at 28 days was slightly lower than the control [52], but this pattern changes with 91 days of normal curing and with hot curing. This can be considered because of the pozzolanic reaction from the GP particles which need more time to react than SF due to their larger size and, therefore, smaller specific surface area. Other researchers confirm this behavior, pointing out that the key to reaching a faster pozzolanic reaction is the GP particle size [3,75], an outcome that reacts better with CH.

The synergy between milled waste glass powder and other mineral admixtures in UHPC has been extensively explored in various studies. Table 5 summarizes some of these endeavors.

**Table 5.** Reported research utilizing waste glass combined with other mineral admixtures in UHPC formulations.

Total Powders (kg/m <sup>3</sup> )	% Cement	% SF	% WGP	Other Mineral Admixture		Other Mineral Admixture		w/b	Compressive Strength (MPa)	Reference
				Type	%	Type	%			
1180–1727	59.88–90.00	6.83–10.00	0.00–27.03	Rejected-FA	0.00–31.67	-	-	0.15	148–158	[48]
1147–1246	58.99–88.13	0.00–11.87	0.00–33.06	QP	0.00–15.42	-	-	0.15–0.25	153–221 *	[42,64]
1151–1282	47.26–63.38	8.76–17.63	19.03–37.73	-	-	-	-	0.15–0.20	100–177	[1]
1035–1052	78.23–78.31	0.00–21.74	0.00–21.77	-	-	-	-	0.21	100–175	[77]
1131–1147	50.05–58.72	8.76–8.84	7.83–13.92	Limestone	20.37–21.01	FC3R	4.38–4.40	0.16–0.18	132–156	[27]
1158–1210	48.80–56.84	8.26–8.63	25.52–31.66	Limestone	7.60–11.25	-	-	0.14–0.16	101–162	[75]
1287	37.95–48.17	7.70	24.08	Limestone	19.98	MK	0.00–10.21	0.16–0.18	129–159	[3]
1190	56.80	11.93	31.26	-	-	-	-	0.18	155	[15]
1282	46.02	7.80	26.13	Limestone	20.05	-	-	0.15	156	[9,10,18,93]
1165–1195	43.24–59.15	8.36–8.58	3.85–18.04	Limestone	21.79–35.96	EAFS	2.19–14.29	0.14–0.16	100–163	[29]
1205–1280	45.55–57.01	7.65–7.80	26.01–33.02	Limestone	10.15–30.22	-	-	0.14–0.21	142–156	[58]
1259	38.80–49.25	7.94	25.23	Limestone	17.58	RHA	0.00–10.45	0.16–0.18	139–159	[94,95]

\* Heat curing conditions.

A multi-criteria optimization technique was carried out to design two eco-friendly UHPCs incorporating micro-limestone powder and two different sizes of GP as cement and SF partial replacements [47,59,75]. The UHPC formulations analyzed, which included a Control dosage without alternative binders, as well as their scheme of pastes' packing density, are presented in Table 6 and Figure 6, respectively. The optimized mixtures exhibited excellent workability and rheological properties, achieving high compressive strength with reduced cement content. Furthermore, new research has corroborated the synergy between glass waste and limestone powders [47,59,96]. Particularly, their joint use demonstrated an improvement in rheology that allowed a reduction in the superplasticizer content and water-to-binder ratios with respect to conventional UHPC dosages. The reductions mentioned carry significant positive implications for the material properties due to two main reasons [94,97]:

- (i). Lowering the w/b ratio drives reduced porosity within the material.
- (ii). Decreasing the superplasticizer content mitigates the risk of potential incompatibility with cementitious materials.

**Table 6.** Control, Optimized 1 and Optimized 2 UHPC formulations [47,59].

	Control	Optimized 1	Optimized 2
OPC (kg/m <sup>3</sup> )	852	590	603
SF (kg/m <sup>3</sup> )	272	100	100
Waste glass powder (kg/m <sup>3</sup> )	-	-	169
Waste glass flour (kg/m <sup>3</sup> )	-	335	199
LP (kg/m <sup>3</sup> )	-	257	118
SS (kg/m <sup>3</sup> )	889	778	834
HRWRA (kg/m <sup>3</sup> )	26.5	21.5	20.0
w/b	0.218	0.165	0.163
Slump flow (mm)	260	253	258
VPD *	0.83	0.81	0.79

\* Virtual Packing Density as per the Sedran &amp; Larrard theory [19,98,99].

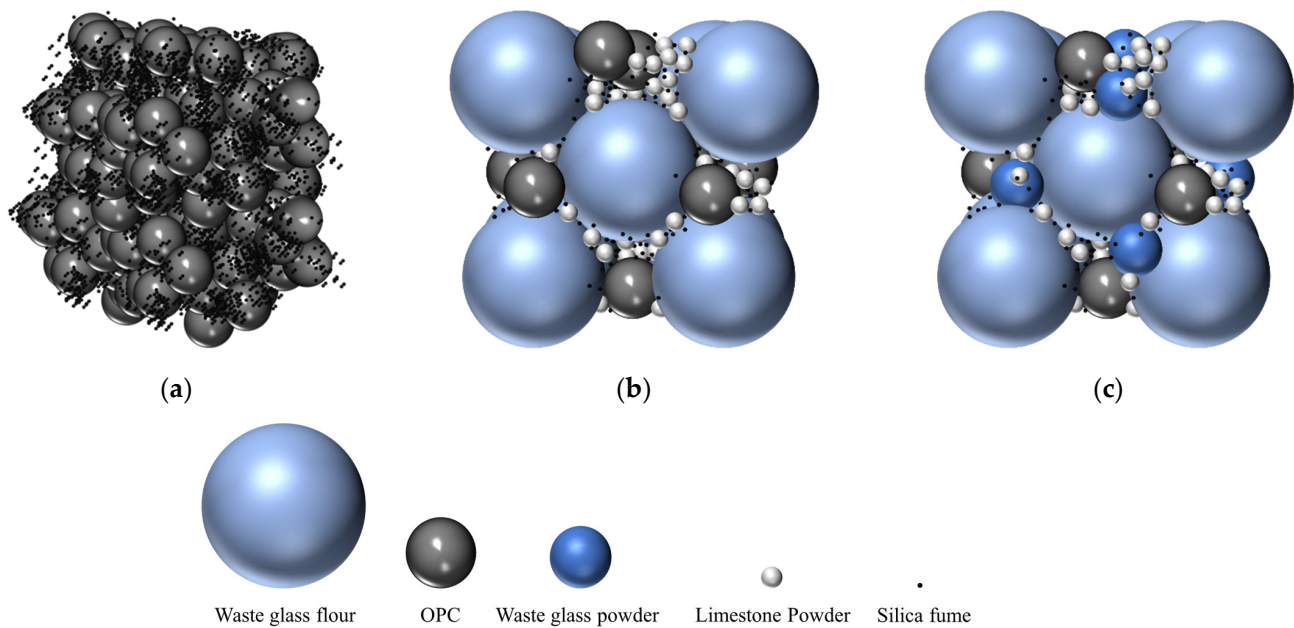


**Figure 6.** Scheme of paste packing density for three UHPC formulations (a) Control mixture without alternative binders; (b) Optimized 1 mixture with micro-limestone powder and waste glass flour ( $d_{50}$ : 28  $\mu\text{m}$ ); (c) Optimized 2 mixture with micro-limestone powder, waste glass powder ( $d_{50}$ : 7  $\mu\text{m}$ ) and waste glass flour ( $d_{50}$ : 28  $\mu\text{m}$ ) [82].

Similarly, [29] investigated the factorial design of an ultra-high strength mortar containing Electric Arc Slag Furnace (EASF) along with milled waste glass. The study highlighted the importance of incorporating supplementary cementitious materials for enhancing both the mechanical strength and sustainability of UHPC. The effect of high reactive aluminosilicates cementitious materials, like metakaolin (MK) and Fluid Catalytic Cracking Catalyst Residue (FC3R), in waste glass-UHPC was explored [3,27]. Due to the reaction of the high alumina-silicate components of FC3R and MK, yielding ettringite formation, those cementitious materials showed potential for enhancing early-age strength, but their impact on long-term strength and workability was observed to vary based on substitution levels. Hence, the findings of these investigations illustrate the collaborative effect of limestone and glass powder in alleviating rheological issues in mixtures containing FR3C or MK. Thereby, with the optimal dosage of these high alumina materials, the effect of glass and limestone allows the UHPC to exhibit beneficial properties for early strength development, all the while maintaining cost-effectiveness, a proper rheology feature in the fresh state, and reducing the carbon footprint [3,27].

The literature review, as depicted in Table 5, highlights another significant aspect concerning the utilization of GP in these specialized concrete formulations. Specifically, UHPC compositions incorporating GP as a partial or complete substitute for QP have exhibited impressive compressive strengths exceeding 200 MPa [42,64]. This threshold value is crucial for ensuring strong fiber-matrix adherence [100,101], emphasizing the promising potential of glass powder in enhancing the performance of UHPC formulations.

For its part, several investigations have focused on the utilization of rejected fly ash along with recycled glass powder in UHPC formulations [28,48]. On the one hand, the research presented in [28] explored the utilization of local high unburned carbon fly ash as a mineral admixture in waste glass-UHPC. On the other hand, research presented in [48] depicted the utilization of fly ash with particles larger than 45 microns along with recycled glass in alternative formulations of UHPC. Despite challenges in achieving optimal substitutions owing to the elevated content of rejected fly ash, these studies emphasized the potential of utilizing local pozzolans for sustainable UHPC production. Lastly, recent studies [94,95] analyzed the effect of rice husk ash (RHA) as a cement partial

replacement for UHPC containing waste glass powder. Despite a decrease in workability, attributed to the high surface area and porous nature of RHA particles which increases water demand [102,103], and a slight reduction in CS, the studies highlighted the potential of RHA for enhancing sustainability and reducing the carbon footprint of UHPC.

Overall, these studies summarized in Tables 5 and 6 underscored the significance of synergistic interactions between waste glass powder and other mineral admixtures in enhancing the sustainability and performance of UHPC formulations. A deeper analysis of the influence of these interactions on each of the material characteristics is presented in the following subsections.

#### 4.2. Waste Glass as a Replacement for QS

UHPC formulations traditionally incorporate quartz sand (QS) as the aggregate, with quartz powder (QP) enhancing mixture density [14,104]. However, QS and QP are known carcinogens, posing health risks to workers and impacting the environment [69,105]. As reported in published research, the replacement of these materials with recycled glass sand (GS) could offer a safer and more sustainable solution [1,49,69,106]. These findings are summarized in Table 7. As can be seen, these studies have explored different replacement ratios and particle size distributions of recycled glass sand, aiming to balance workability and mechanical properties [41,69]. Notably, UHPC formulations with GS have demonstrated exceptional compressive strengths exceeding 200 MPa under thermal curing conditions [1]. These results suggest the potential of GS in UHPC as a viable alternative for even the highest levels of improved microstructure (identified by CS greater than 190 MPa) which indicates a possible exceptional fiber-matrix adhesion [100,101].

**Table 7.** Results of compressive strength of UHPC with glass sand.

Glass Sand $d_{50}$ ( $\mu\text{m}$ )	Glass Sand $d_{\text{max}}$ ( $\mu\text{m}$ )	Quartz Sand Replacement Percentage (%)	Compressive Strength Normal Curing (MPa)	Compressive Strength Heat Curing (MPa)	Reference
275	630	50	171 ***	196 *	[69]
275	630	100	157 ***	182 *	[69]
350	630	100	128 ***	153 *	[69]
225	630	100	127 ***	164 *	[69]
300	600	100	124 **	-	[50]
-	800	25	175 ***	200 *	[1]
-	800	50	165 ***	190 *	[1]
-	800	50	162 ***	175 *	[1]
275	630	50	140 ***	150 *	[106]

\* After 2 days of heat curing; \*\* after 28 days of normal curing; \*\*\* after 91 days of normal curing.

Additionally, research on alternative glass UHPC formulations revealed that varying combinations of glass components, such as GP, fine glass powder (FGP) and GS, significantly influenced workability and mechanical performance, with CS values of up to 171 MPa observed even under normal curing conditions [77].

Moreover, the study conducted by [49,50] showcased the highest proportion of recycled glass utilization in UHPC formulations. These formulations replaced 100% of quartz sand with GS and incorporated various sizes of GP, resulting in up to 52% of the mixture by weight being comprised of recycled glass (both sand and powder). Finally, it is important to note the risk of ASR associated with glass sand [91], which will be addressed in a specific section of the review article.

## 5. Effect of WG Addition on UHPC's Features

### 5.1. Rheological Properties

Concrete's rheological properties are a measure of its ability to flow and resist deformation. In the case of UHPC, rheological properties are especially important due to the high particle density and low w/b [97,107]. The utilization of GP as a supplementary

cementitious agent can significantly improve these properties of UHPC [40,62,96]. In this sense, the research conducted by [75] revealed that replacing some of the cement with GP in UHPC formulations leads to a higher spread flow due to the glass powder's minimal water absorption and the consequently higher alkaline content resulting from the recycled glass's elevated  $\text{Na}_2\text{O}$  levels [75]. The high-level alkali essence and the low water absorption of glass particles are well known, and they are depicted in Tables 2–4 of the present document. On the one hand, utilizing GP in cement partial replacement capitalizes on its significantly lower water absorption [1,69], thereby liberating more free water to effectively contribute to the material's rheological behavior in its fresh state [58,75]. On the other hand, the alkalinity provided by GP can enhance the performance of superplasticizers in cement pastes by facilitating the dispersion of cement particles and reducing their agglomeration. This improved dispersion allows the superplasticizer molecules to effectively adsorb onto the cement particles, leading to better fluidity and workability of the paste [108].

The impact of incorporating GP into the mixture on UHPC's rheology is evident in Figure 7 [12]. On the left, the slump flow of a blend devoid of recycled glass is depicted, whereas the image on the right illustrates the outcome following the substitution of 13.5% of the cement with GP. It is notable that the mixture lacking GP exhibits a slump flow of 210 mm, while the addition of GP results in a higher slump flow of 250 mm, despite maintaining the same  $w/b$  ratio and dosage of high-range water-reducing polycarboxylate-based superplasticizer (HRWR) ( $w/b = 0.165$  and HRWR dosage of  $23 \text{ kg/m}^3$ ).

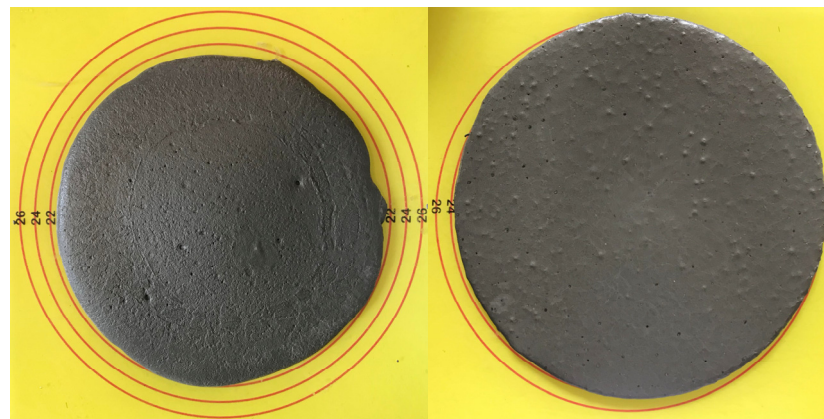


**Figure 7.** Impact of GP on UHPC's rheology. The left image shows the slump flow of a GP-free mixture, contrasting with the right image depicting the effect of replacing 13.5% of cement with GP [12].

Other studies have assessed the UHPC mechanical and rheological features incorporating varying proportions of glass powder as a pozzolanic mineral admixture [1,41,63]. Their findings indicated that the GP addition enhanced workability and flowability without compromising strength and durability. Notably, the incorporation of glass powder mitigated exudation and bleeding, thereby improving bonding capacity and resistance to segregation. Finally, the positive influence of recycled glass together with limestone is observed in Table 6, which shows that thanks to the incorporation of these components in cement and SF partial replacement, the optimized dosages achieve the same value of slump flow as the Control mix, but with a lower  $w/b$  value and lower superplasticizer content [47,59].

## 5.2. Hydration Kinetics

Comprehending the hydration is vital for understanding the behavior of cementitious materials, particularly in the context of advancing UHPC [41]. The study delved into the cement hydration kinetics, focusing on the influence of GP addition, using isothermal calorimetry to examine the pozzolanic reaction during the cement hydration early stages [41]. The investigation scrutinized the rate at which UHPC emits heat during hy-

dration and the cumulative heat curves of hydration for varying levels of glass powder replacement (0%, 20%, 40% and 50%) within the initial 48 h of water-cementitious material contact, normalized to the total binder weight in the mixture. It became apparent that both the maximum heat flow and total heat decreased with increasing GP replacement ratios. Moreover, the study revealed that the maximum value of the second exothermic peak decreased by 35%, 32% and 50% for the mixtures containing 20%, 40% and 50% glass powder, respectively, in comparison with a typical UHPC. The decrease in heat release was attributed, on the one hand, to the dilution effect caused by the incorporation of glass powder, which, in the reported research, possessed a lower specific surface area than cement [41]. On the other hand, the GP pozzolanic reaction produces less heat than ordinary Portland cement due to its similarity to a C2S reaction [109]. This lower heat of hydration aided in minimizing cracking as a consequence of the elevated temperatures [41].

Moreover, when GP replaced 20% of the cement, the end of the induction period and the acceleration period ascribed to the major peak were shorter [41]. This acceleration was explained by the ability of fine GP to expedite the hydration of cement by adsorbing calcium ions and acting as nucleation sites for hydrate formation. Additionally, the high alkali content in GP was probed to catalyze the early formation of C-S-H [41]. Conversely, with GP replacement of over 20%, the periods of induction and acceleration were delayed. For instance, at the end of the induction period for typical UHPC formulation, and formulations with 40 and 50% cement replacement by GP were about 9.1, 9.7 and 11.2 h, respectively. This delay was attributed to increased levels of GP replacement, resulting in higher water-to-cement ratios and superplasticizer dosages, as is common in UHPC manufacturing [41]. This, according to Jansen et al. [110], could lead to the complexation of  $\text{Ca}^{2+}$  ions by the superplasticizer, impeding the early hydration of cement and delaying the pozzolanic process owing to the insufficient CH presence in the concrete.

### 5.3. UHPC's Microstructure

The cement-based materials' mechanical properties are influenced by various factors, such as their chemical characterization, microstructure, aggregate features and the ITZs characteristics [21,111]. Understanding the microstructure of these matrices is key to unraveling their mechanical behavior. Although UHPC presents a highly heterogeneous and intricate microstructure, efforts to create realistic models remain challenging [112–114]. Nevertheless, delving into the microstructure of UHPC allows for the determination of optimal mix compositions, which in turn yield desirable fresh and mechanical properties and enhanced durability, thereby reducing production costs and related  $\text{CO}_2$  emissions [56,113,115].

Therefore, microstructure analysis procedures like X-ray diffraction (XRD), scanning electron microscopy/energy-dispersive spectroscopy (SEM/EDS), mercury intrusion porosimetry (MIP),  $^{29}\text{Si}$  magic-angle sample-spinning nuclear magnetic resonance ( $^{29}\text{Si}$  MAS NMR) analysis and thermogravimetric/differential thermal analysis (TG/DTA) have been extensively reported in the literature as methodologies to gain insights into the microstructure of UHPC [41,64,116]. In this sense, studies on UHPC microstructure indicate that incorporating cement partial replacements like limestone and granulated blast furnace slag not only reduces unhydrated cement content and the C2S/C3S ratio but also diminishes CH levels while promoting the creation of C-S-H, resulting in a more compact and homogeneous cementitious matrix. Among the various pozzolans assessed, silica fume stands out for its ability to decrease porosity, lower the calcium/silicon (Ca/Si) ratio and maintain minimal CH levels, all contributing to defining optimal mechanical specifications for UHPC. Furthermore, the inclusion of blast furnace slag, electric arc furnace slag and limestone powder as mineral admixtures aids in further reducing UHPC matrix porosity and allows for a reduction in cement consumption. While each substitute offers specific advantages, their optimized use strengthens the mechanical or maintains (depending on the case) the final properties of UHPC while supporting sustainable waste management practices [21,29,56,117].

Additionally, integrating nano-silica as a cement replacement presents a promising avenue to enhance the mechanical characteristics of UHPC further. Nano-silica fosters the formation of a denser matrix with reduced porosity and increased C-S-H content [117]. Hence, considering the properties of recycled glass discussed in earlier sections (e.g., chemical composition and crystallography), it is reasonable to anticipate that the addition of GP in UHPC formulations would yield a beneficial influence akin to that of reported mineral admixtures. Soliman & Tagnit-Hamou [41] conducted some research to analyze the influence of the cement and/or quartz powder partial replacements with glass powder— with  $d_{50}$  equal to 50  $\mu\text{m}$ —on the UHPC's microstructure by utilizing SEM approaches. Three samples were evaluated: (i) a control one, which represented a typical UHPC formulation; (ii) 80C/20GP formulation in which the 20% of the weight of cement was replaced by GP; and (iii) 0QP/100GP in which QP was totally replaced by GP. Their findings using backscattered electron (BSE) images revealed that the ITZ in the control mix was thin, and the addition of GP did not significantly affect it. Moreover, owing to the low w/b value, a considerable amount of unreacted cement, QP particles and GP particles were observed in the matrix. The study also revealed that the absence of portlandite (CH) indicated its consumption by the SF plus GP pozzolanic effects. Another conclusion that can be drawn from their BSE research is that the design of the UHPC promoted a dense and homogeneous matrix with reduced porosity, with the presence of spherical air voids being a consequence of the high superplasticizer content. Moreover, BSE images after thermal treatment revealed the formation of a C-S-H hydration layer around the cement and GP particles, demonstrating the pozzolanic reaction of GP and its contribution to the improved microstructure [118–120]. Regarding the characteristics of GP particles, it was observed that their appropriate fineness prevented the formation of microcracks associated with the ASR reaction. Their study proved that the incorporation of GP yielded the formation of more C-S-H, thereby improving the microstructure of UHPC. In addition, their findings also revealed that the presence of GP particles did not adversely affect the ITZ or increase porosity, suggesting adequate compatibility between GP and the cement matrix. This highlights that GP can be an effective additive for enhancing the properties of UHPC without compromising its internal structure [41].

For their part, Vaitkevicius et al. [64] carried out a study to investigate the effects of GP as a complete replacement for QP and SF in UHPC formulations. Through experimental analysis using techniques such as MIP, XRD and  $^{29}\text{Si}$  MAS NMR, the study elucidated the beneficial reactions of GP with cement phases, leading to the formation of C-S-H and subsequent enhancements in mechanical strength and microstructure. Notably, the research highlighted the elimination of macroporosity, increased cement dissolution rate, and the role of fast soluble alkali from the surface of GP in accelerating cement hydration.

#### 5.4. Mechanical Properties

Building on the insights gleaned from earlier sections regarding its effects on rheology, kinetics and microstructure, the incorporation of glass powder into UHPC is anticipated to yield enhancements or minimal reductions in its mechanical features. Nevertheless, the following sections of this review article will analyze the impact of the addition of GP in the UHPC formulations on their CS, elasticity modulus, ultrasonic pulse velocity, bending performance and direct tensile behavior.

##### 5.4.1. Compressive Strength

The effectiveness of WG powder in enhancing the CS of concrete, particularly in UHPC mixtures, has been extensively explored [55,58,117]. Some of these results are presented in Table 8. The role of GP on the CS of concrete is a consequence of different mechanisms. For instance, the implementation of a particle size of GP finer than cement particles reduces mixture porosity due to the filler effect as a replacement for cementitious materials, leading to a trend of increasing CS. Specially, these fine particles of glass also promote the cement hydration in a UHPC mixture by increasing the hydration surface-volume ratio and the filler

effect, thus producing more hydration products owing to the pozzolanic reactions of fine glass and increasing the creation speed of hydrates that improve the concrete's CS [40,41,51]. In addition, this pozzolanic reaction of glass is due to the amorphous silica composition (as seen in Table 3 and Figure 2) that reacts with CH producing secondary C-S-H gel that mostly provides this mechanical property [120]. Hence, researchers have investigated various sizes and replacement percentages of GP, revealing notable effects on concrete strength [40,41,77]. For instance, studies have applied GP with a  $d_{50}$  particle diameter of 10  $\mu\text{m}$ , replacing 25% of the cement, leading to UHPC exhibiting compressive strength values ranging from 150 to 200 MPa after 91 days of standard curing conditions [40]. Similarly, investigations utilizing GP with a particle size of 12  $\mu\text{m}$  as a partial cement replacement in UHPC with a water-to-binder ratio of 0.189 demonstrated a significant increase in CS, reaching up to 204 MPa at 91 days under normal curing conditions [41].

**Table 8.** Results of WGP application in UHPC compressive strength from 28 to 91 days of SC.

Replaced Material	Percentage of Replacement (%)	GP Fineness $d_{50}$ ( $\mu\text{m}$ )	Concrete Strength Trend	Reference
Cement	20	12	Increase of 13%	[41]
Cement	50	12	Decrease of 9%	[41]
Cement	25	10	Increase of 11%	[40]
Silica Fume	30	3.8	Increase of 8%	[77]
Silica Fume	50	3.8	Increase of 1%	[77]
Silica Fume	100	3.8	Decrease of 16%	[77]
Quartz Powder	100	12	Increase of 17%	[41]
Quartz Powder	50	12	Increase of 11%	[41]
Quartz Powder	100	10	Increase of 19%	[40]

However, as shown in Table 8, substitution ratios of cement with GP exceeding 25% were found to be ineffective, leading to a reduction in the CS [40,41,51]. This phenomenon can be attributed to the delicate balance between two key factors in the UHPC matrix: the creation of portlandite during cement hydration and the pozzolanic activity of glass powder [83]. This way, when a relevant cement portion is replaced with GP, the amount of portlandite generated may decrease due to the reduced cement content, which can lead to several of the pozzolanic materials remaining unreacted [75]. For its part, the lowering of cement also leads to a decrease in the primary C-S-H gel obtained by cement hydration [61,62]. Therefore, the decrease in compressive strength observed at higher replacement ratios of cement with GP suggests that the pozzolanic activity of the glass powder may not fully compensate for the decrease in C-S-H from cement hydration for the reduction in portlandite content.

Furthermore, studies have explored the use of GP as a partial or complete substitution for SF and quartz powder QP in UHPC mixtures. When it comes to the case of silica fume, fine GP, with  $d_{50}$  values of 3.8  $\mu\text{m}$ , was applied as a partial and complete replacement for SF in a UHPC formulation [74]. The findings for UHPC compressive strength are provided in Figure 8. According to the reported study results, and as can be seen in Table 8, replacements of over 50% lead to a decrease in the CS value. The reason for that could be explained by the following: (i) the improvement of the packing density provided by the reduced size of SF, with  $d_{50}$  values of 0.15  $\mu\text{m}$ , can not be attained with glass particles. A proof of the latter can be observed in Table 6, where the VPD of the Control formulation is higher than those of the optimized values [47,59]; (ii) the improved pozzolanic nature of SF than GP, due to its reduced size and higher amorphous silicon oxide [59,63,121].

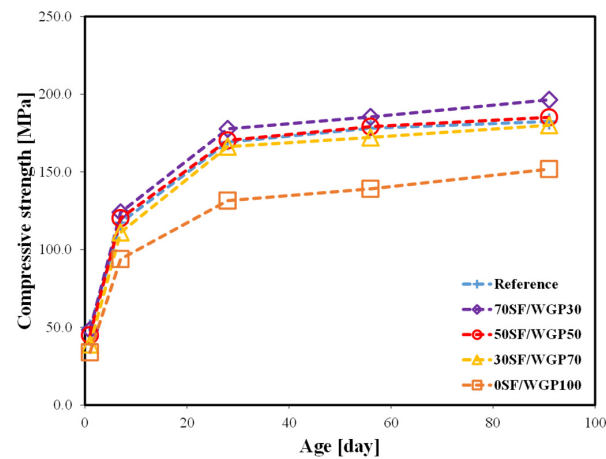


**Figure 8.** Results of UHPC CS of silica fume replacement with fine  $d_{50}$  3.8 GP [77].

Moreover, in another study, glass powder (GP) was introduced as a substitute for QP in a UHPC mixture with a w/b value of 0.189 [41]. The complete replacement of QP with GP led to an enhancement in the compressive strength of the concrete, ranging from 30 MPa to 35 MPa after 91 days of standard curing (SC). The pozzolanic reaction between waste glass powder and cement-hydrated products facilitated an accelerated hydration process, consequently augmenting the strength of the UHPC [40,41].

#### 5.4.2. MoE

The modulus of elasticity is a measure of the stiffness or ability of a material to resist deformation under applied loads. In the case of UHPC, according to the ACI-239R, its value evaluated after 28 days is commonly within the range of 40 to 50 GPa [122]. UHPC's MoE can vary depending on factors like material composition, particle size and distribution, density and porosity [123]. However, in general, the modulus of elasticity of UHPC is much higher than that of other types of concrete, due to its stiffness and the fact that it can withstand larger loads before permanently deforming [123,124].

Jaramillo-Murcia et al. [58] analyzed the modulus of elasticity of two alternative UHPC formulations that incorporated waste glass in their composition. To establish comparisons, a typical UHPC formulation was also tested. The information on the considered formulations can be observed in Table 6 while and scheme of their paste's structure is presented in Figure 6. The findings of this study, measured at different ages, are put forward in Figure 9.

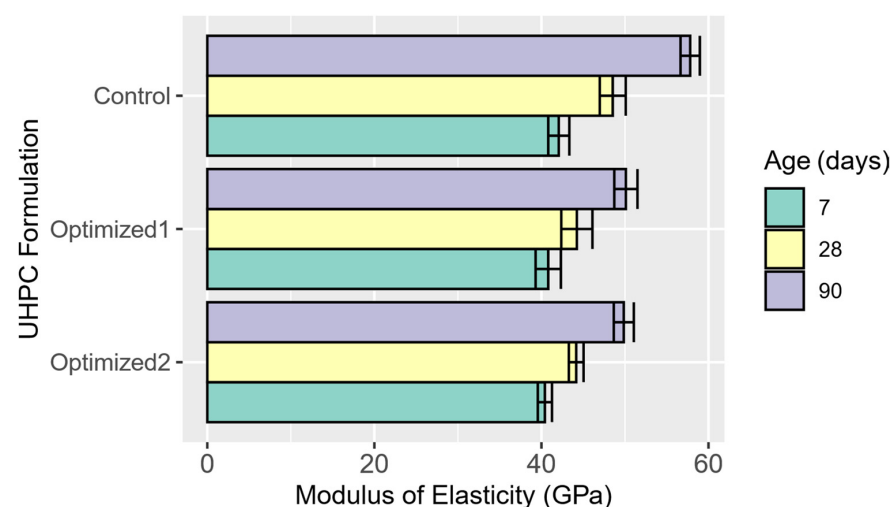


**Figure 9.** MoE of control and optimized UHPC formulations evaluated at 7, 18 and 90 days [58].

Throughout their study, it was noticed that the Control formulation consistently exhibited a higher Modulus of Elasticity (MoE) compared to the waste glass formulations at each stage. Nevertheless, all examined UHPC formulations met the Modulus of Elasticity criteria outlined by ACI 239 [5]. The rate of MoE increase over curing time varied among formulations containing different supplementary cementitious materials [125]. Incorporating pozzolans with higher activity, such as SF, resulted in accelerated enhancement of MoE during the initial stages due to their smaller particle size and faster hydration kinetics. Additionally, the improved packing density of the Control mix contributed to its improved MoE. Nevertheless, differences observed in younger specimens were slightly less marked in comparison with the older ones. This could be attributed to the influence of limestone powder and GP, which, as suggested by previous studies [12,75], speeds up the hydration process in the early stages, driving denser particle structures and enhanced mechanical properties. Moreover, the GP addition was found to expedite the cement dissolution rate, thereby facilitating a faster hydration process, as stated in previous sections [40,41,51].

#### 5.4.3. Ultrasonic Pulse Velocity

Upon analyzing the ultrasonic pulse velocity data, on the same three UHPC formulations presented in the previous section, Jaramillo-Murcia et al. [58] reported a consistent upward trend in values over time. Figure 10 depicts the results obtained by [58] in relation to this property. Notably, as Figure 10 reveals, the Control mixture exhibits the highest response, followed by the Optimized 2 mixture. The authors attributed this increase in velocity to the VPD of the UHPC's formulations (see Table 6), resulting in increased stiffness of the material and accelerated pulse wave propagation within the UHPC cylinder. Consequently, as per their findings, the ranking of UHPC types as per their VPD values corresponds to the dosages determined by their ultrasonic pulse velocity at any given age. Moreover, this research also suggests a significant correlation between velocity enhancement and the reactive powders' hydration and pozzolanic activities [58].

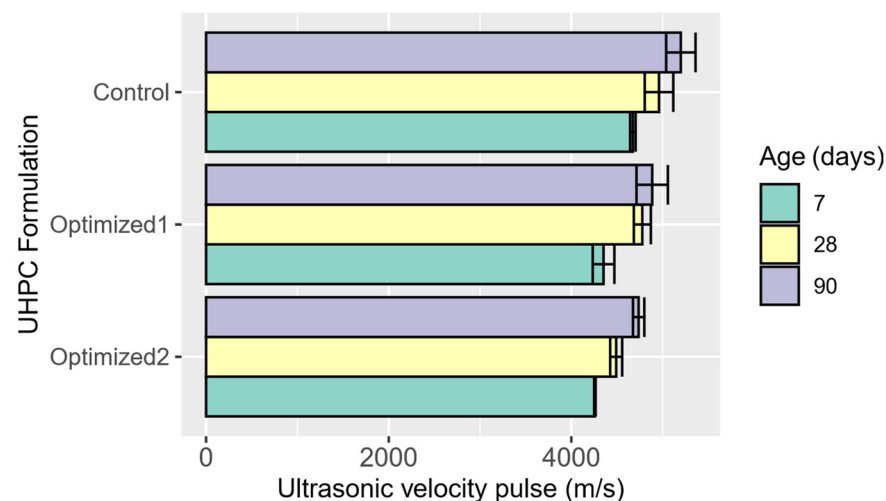


**Figure 10.** Ultrasonic pulse velocity findings of control and optimized UHPC formulations evaluated at 7, 18 and 90 days [58].

The study also established that concrete of superior quality typically exhibits an ultrasonic pulse velocity exceeding 4575 m/s. As illustrated in Figure 10, the Control dosage reaches the threshold value after seven days of curing, while Optimized 1 requires 28 days, and Optimized 2 necessitates 90 days to achieve a similar threshold value. It is worth mentioning that the mix in Optimized 2 at 28 days achieves a UPV value of 4491 m/s [58].

#### 5.4.4. Flexural Behavior

The literature review shows that substituting some of the Portland cement with GP diminishes the resistance to bending in plain UHPC formulations [15,62]. However, while it is notable that the flexural strength lowers with increasing substitution of GP in the case of plain UHPC, it is important to recognize that in fiber-reinforced UHPC, the primary determinant of performance is the fiber reinforcement system [126–128]. Neira-Medina et al. [15] researched to analyze the impact of different fiber-reinforced systems on the flexural behavior of UHPC utilizing a GP as a cementitious material. The UHPC cementitious matrix was characterized by a w/b value of 0.25, and glass powder with a  $d_{50}$  value of 10  $\mu\text{m}$  was utilized as a cement replacement at a rate of substitution by weight of 45%. The mix design was formulated based on fractal-based particle-packing theories [15]. The experimental campaign included four types of commercial synthetic fibers, both macro and micro, along with high-strength steel fibers, for evaluation purposes. In addition, the fiber reinforcement system encompassed mono and hybrid systems with volume ratios of reinforcement from 1 to 2%, whose results are depicted in Figures 11 and 12, respectively. Notably, only the UHPC specimens reinforced with 2% fibers demonstrated ductile behavior, with the exception of the beam reinforced with 1% steel microfibers [15].

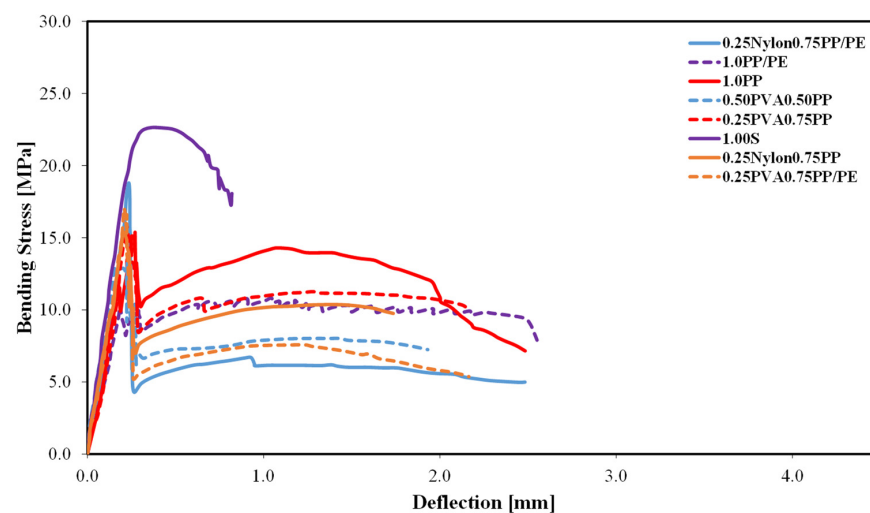


Figure 11. Effect of 1% of fibers on the waste glass-UHPC flexural behavior [15].

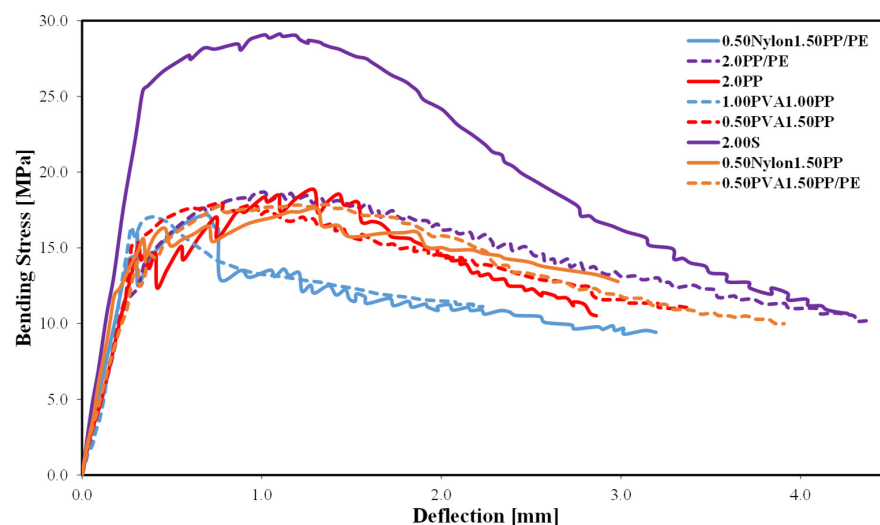
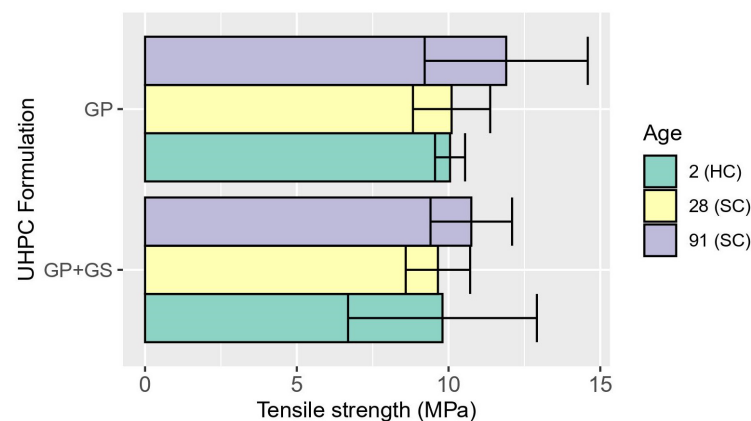


Figure 12. Effect of 2% of fibers on the waste glass-UHPC flexural behavior [15].

Moreover, it is important to note that the performance of series reinforced with 1% and 2% high-strength steel fibers (represented as 1.00S and 2.00S in Figures 11 and 12) achieved results comparable to those reported for the same reinforcement in traditional UHPC matrices without recycled glass. Among these pieces of research with typical UHPC matrices and similar limits of proportionality and modulus of rupture when using 1% or 2% of OL 13/0.20 fiber, the following references can be consulted [129–131].

#### 5.4.5. Tensile Behavior

Mousa et al. [106] studied the tensile behavior of UHPC through the utilization of GP and GS as replacements for cement and fine aggregates, respectively. This study compares two distinct UHPC compositions: one incorporating GP as a cement substitute, and the other integrating both GP and GS. Both mixtures featured a 2% volume fraction of OL 13/02 steel microfibers with an aspect ratio of 65. In addition, the research explored the influence of two curing regimes, hot curing and normal curing, on the tensile behavior of the recycled glass UHPC samples at the ages of 28 and 91 days. A significant experimental factor considered was the alignment of the steel microfibers (either parallel or perpendicular to the fracture plane). Fiber orientation was induced during the pouring procedure. The trials were conducted following the technique known as the Double Edge Wedge Splitting Test (DEWS) [132]. Figure 13 shows the graphs with the results obtained in the specimens with fibers aligned perpendicular to the fracture [106]. It is noteworthy that these results are the only ones that could be corroborated with those obtained from dogbone specimens, as the use of dogbone specimens, owing to their gauge dimensions, promotes a favorable orientation of the fibers [101,133].



**Figure 13.** Maximum tensile stresses of UHPC mixtures with only glass powder (GP) or glass powder and glass sand (GP+GS) after 2 days of heat curing, and 28 and 91 days of standard curing (SC) [106].

As can be observed in Figure 13, both cementitious matrices achieved excellent tensile strength [106], in the same range as those achieved with standard UHPC reinforced with a 2% OL 13/0.2 fiber [123,133–135]. Another conclusion that can be drawn from this figure is the improvement in the CS between 28 and 90 days of standard curing (SC) which may be attributed to the slow pozzolanic reaction of glass powder [61,92]. Finally, it is relevant to denote that, the results obtained in the specimens with fibers aligned parallel to the fracture were about half of those presented in Figure 13 [106].

Nevertheless, the most relevant feature of UHPC is not its maximum tensile strength, but its direct tensile performance [10,100,136]. The introduction of fibers not only augments the material's tensile strength but, with the proper dosage of adequate fibers, also facilitates efficient force transfer even in the presence of cracks, thereby impeding or decelerating their propagation [137,138]. Fibers within the fissures serve to convey a portion of the matrix's tensile strength, enabling the composite to endure greater strains under favorable circumstances [11,138]. This state is achieved through the strategic alignment of a sufficient number of fibers possessing proper properties within the cementitious matrix [139].

In strain-hardening UHPC, the fiber-reinforced composite demonstrates the capacity to withstand stress increments beyond its cracking stress ( $\sigma_{cc}$ ) until it reaches its maximum peak stress ( $\sigma_{pc}$ ) [18,140]. Figure 14 depicts the various phases of the stress-strain curve for a strain-hardening UHPC under uniaxial tensile loading [106]. These stages encompass the elastic phase, multicracking phase, crack-straining phase and strain-softening phase. Initially, the material experiences elastic deformation until it reaches the point of tension, known as  $\sigma_{cc}$ , and attains a strain of  $\varepsilon_{cc}$ . Beyond this point, the material enters the inelastic strain zone characterized by repeated micro-cracking, surpassing the  $\sigma_{cc}$  tension, with stress levels remaining relatively stable [11,106]. Subsequently, the crack-straining phase ensues, marked by a significant increase in crack opening as the fiber reinforcement undergoes debonding and elastic straining, contingent upon the fiber type [101]. This branch extends until it reaches the maximum stress  $\sigma_{pc}$  and strain  $\varepsilon_{pc}$  [139].

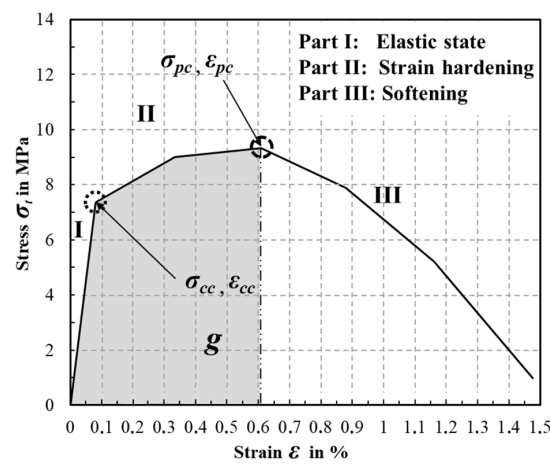


**Figure 14.** Phases of the uniaxial stress-strain curve for a strain-hardening UHPC [93].

In Figure 14, the energy absorption capacity ( $g$ ) of the material can be computed as the area below the strain-stress curve until reaching the stress level denoted by  $\sigma_{pc}$  and  $\varepsilon_{pc}$  [18]. Subsequently, in the third step, a notable decline in the fiber-reinforced UHPC strength develops as the strain increases, a phenomenon known as the strain-softening branch. During this phase, specimen failure is attributed to the slippage and/or rupture of fibers within critical fissures [20,106].

Abellán-García [12,93] investigated the ductility performance of uniaxial tensile behavior across 52 different series of recycled glass UHPC tests. His research focused on a recycled-glass cementitious matrix, particularly examining its suitability for seismic retrofitting applications. The experimentation encompassed various fiber types, including both steel and synthetic options, whose descriptions are presented in Table 9. It is also worth noticing that the  $S_1$  fiber utilized in these studies corresponds to the smooth and high-strength steel OL 13/02 fiber.

**Table 9.** Detailed description of the fibers reported by [93].

Notation	Form	$d_f/l_f$	Material	Strength (MPa)
$S_1$	Smooth	65	Steel	≈2600
$S_2$	Smooth	30	Steel	≈2600
$H_1$	Hooked	70	Steel	≈2000
$H_2$	Hooked	80	Steel	≈1600
PP	Twisted	26	Steel	≈1700
PE	Corrugated	75	Polypropylene	≈650
PVA	Fibrillated	67	Polyethylene	≈550

Figure 15 presents the multicracking pattern in a strain-hardening glass-UHPC specimen reported in reference [12]. Some of the strain stress curves of strain hardening glass UHPC developed in [12,93] are presented in Figure 16.

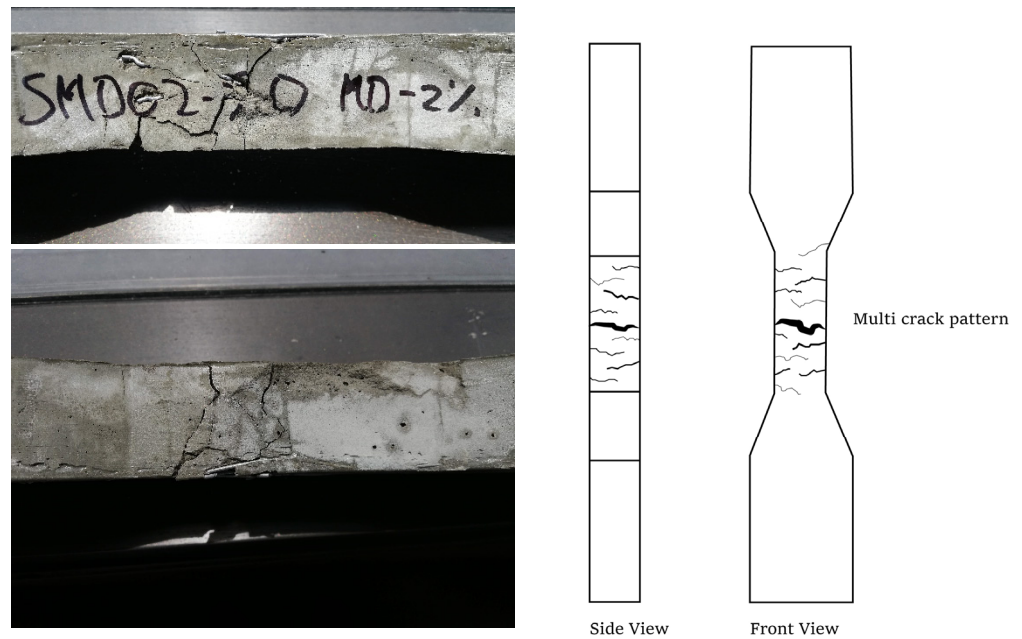


Figure 15. Recycled glass UHPC specimens with strain hardening behavior after failure. Detail of multi crack pattern [12].

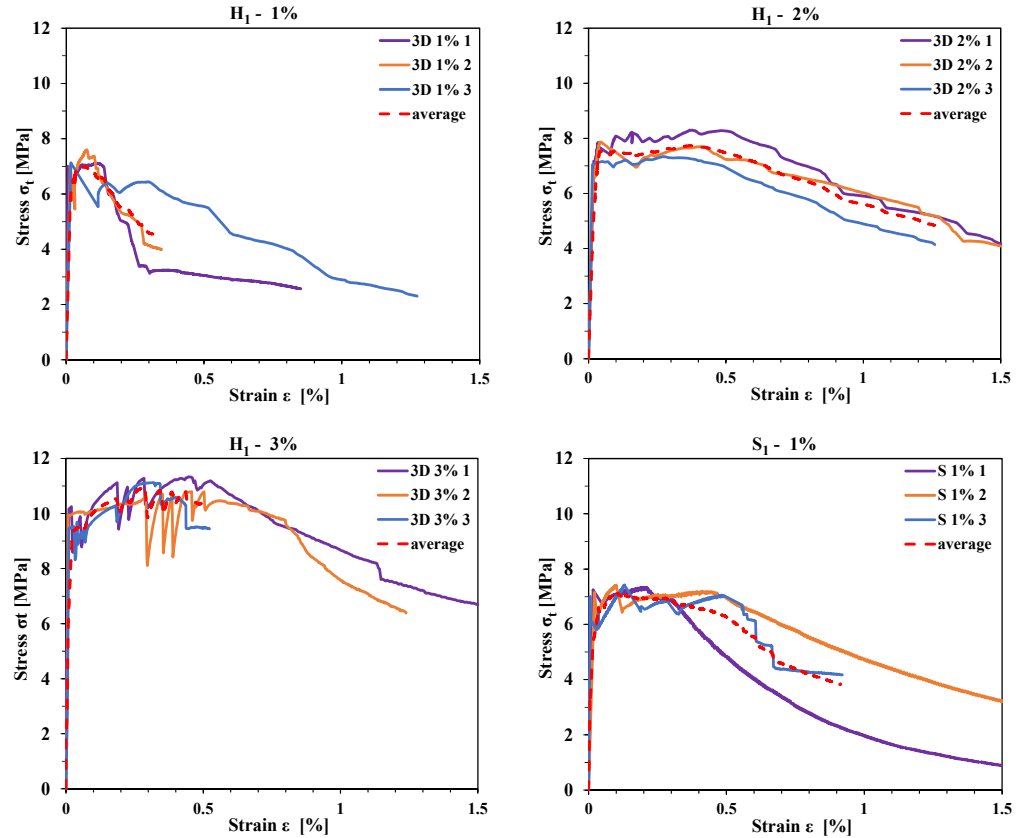
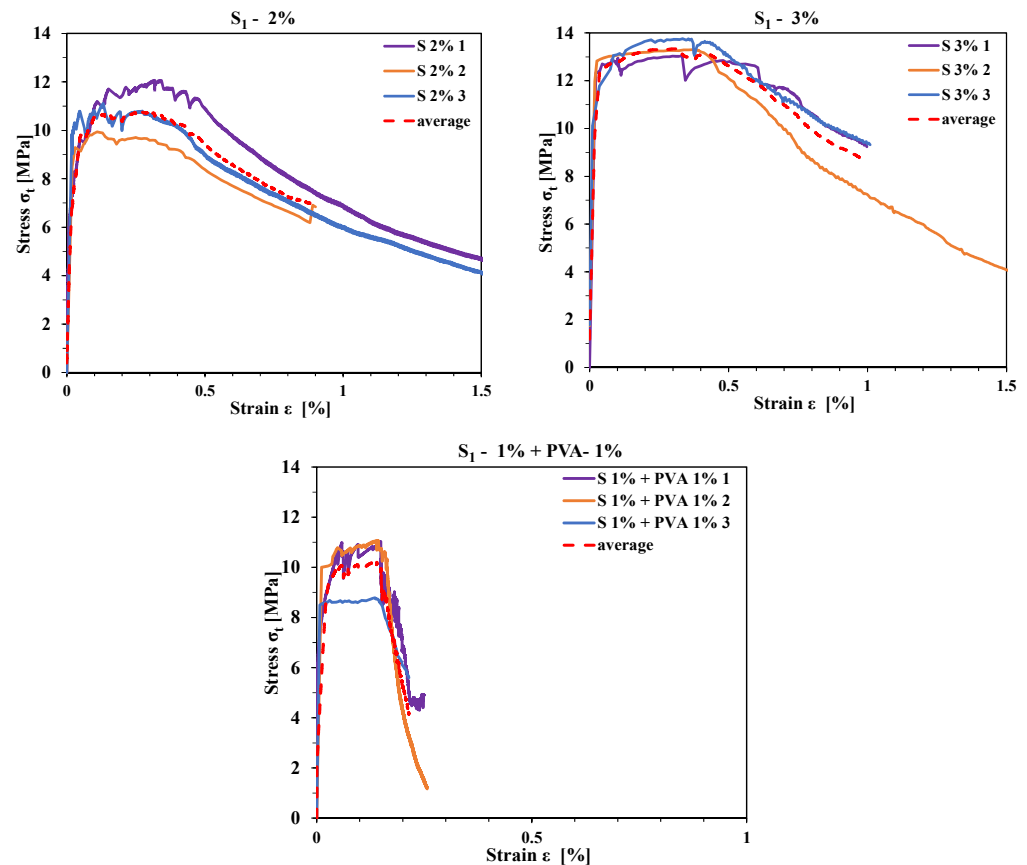


Figure 16. Cont.



**Figure 16.** Direct traction stress-strain graphs [93].  $H_1$  represents hooked steel fiber;  $S_1$  represents smooth steel fiber; and PVA represents polyvinyl alcohol fiber.

Among the conclusions drawn from these studies, it is notable that the ductility parameters achieved with the glass cementitious matrix closely approximate those reported in studies employing conventional UHPC matrices [93,96]. For instance, the waste glass–UHPC reinforced with a 2.0% volume fraction of OL 13/0.2 fibers exhibited a peak post-cracking strength of 11.03 MPa, only marginally lower than the 11.30 MPa reported in previous research, with a strain of 0.20% compared to 0.19%. The performance achieved, despite reducing cement content by approximately 35% and silica fume by 50%, can be attributed to the chemical and physical properties of micro-limestone and recycled glass powder [10,93,96]. These materials facilitated substantial substitution of the typical UHPC-making constituents without significantly compromising the chemical balance and packing density of the matrix.

### 5.5. Durability Properties

This review investigates the effect of GP on UHPC’s durability by analyzing several key properties reported in existing literature. These properties include voids in hardened concrete, chloride penetration, initial surface absorption, freeze-thaw performance, ASR, mechanical abrasion resistance, drying shrinkage and resistance to deicing salt scaling.

#### 5.5.1. Voids in Hardened Concrete

In their study, Jaramillo-Murcia et al. [58] presented compelling findings regarding void measurements in hardened concrete, following the ASTM C642 procedure, comparing the results of a Control UHPC mixture, without any alternative SCMs, with two optimized mixtures that incorporate recycled glass as mineral admixtures. More information about these dosages can be found in Table 6 and Figure 6. The reported results, measured at different ages, are illustrated in Figure 17. Their investigation revealed that all UHPC mixes

consistently exhibit low void content throughout the curing process. This way, by the seventh day of curing, samples demonstrate void content below 5%, indicating a promising trend that persists with advancing treatment time.

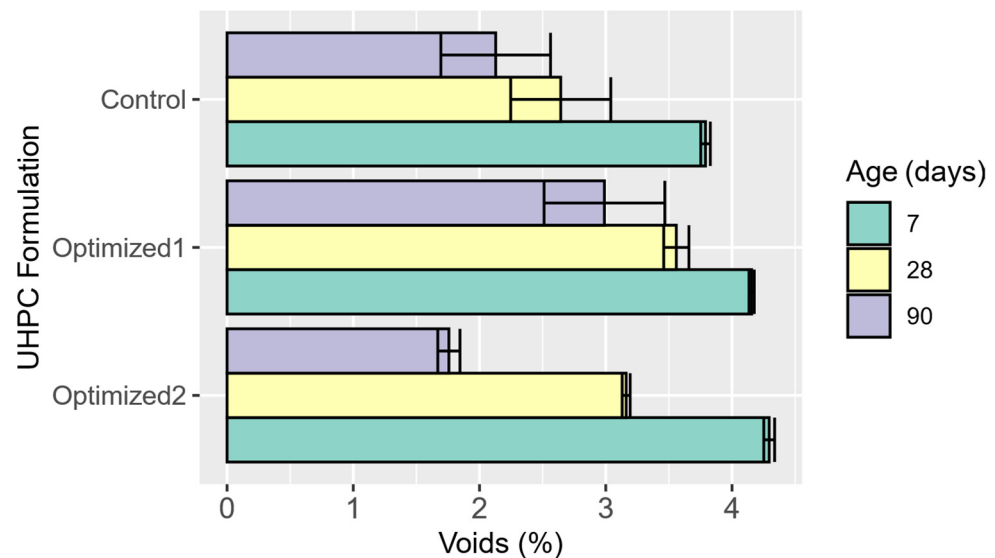


**Figure 17.** Findings in voids in hardened concrete measured by Jaramillo-Murcia et al. [58] at different ages.

Of particular interest is the exceptional performance of the Optimized 2 mixture, surpassing even the Control mixture by the 90-day mark. This noteworthy discovery highlights the positive impacts of the investigated admixtures, attributed to the development of C-S-H gel facilitated by the interaction of CH crystals with SF and GP particles [58]. Furthermore, Jaramillo-Murcia et al. [58] shed light on the implications of silica fume particle content in the Control mixture, which necessitates a higher water dosage, potentially contributing to increased internal fracturing. Their findings suggest a correlation between reduced silica fume content and mitigated drying shrinkage, thereby minimizing the risk of microcracking. These findings are also aligned with [12,141]. The study observes that the Optimized 2 mixture requires the lowest water dosage, a phenomenon attributed to the elevated alkali content in this formulation, synergistically enhanced by both types of glass powders. The effect of alkali content in rheology was previously explained and has been widely reported by [75,108,142], whose results underscore the intricate relationship between material composition and superplasticizer efficacy.

### 5.5.2. Chloride Penetration

As per Nancy Soliman et al. [40], in the realm of UHPC, the incorporation of recycled GP introduces a notable enhancement in resistance to chloride-ion penetration. As per these authors, the dense matrix inherent to UHPC serves as a critical barrier against the ingress of detrimental materials, effectively sealing the structure and bolstering its durability. Therefore, Soliman's findings reveal that UHPC formulations containing recycled glass powder exhibit remarkably low levels of chloride-ion penetration, with average total Coulombs passed values of 5.0 and 3.0 at 28 and 91 days, respectively. These findings align with the "negligible" classification as per ASTM C1202 standards, underscoring the effectiveness of the dense matrix in mitigating chloride ingress [40]. By comparison, traditional UHPC formulations subjected to standard heat treatment demonstrate significantly higher total charge passed values, reaching 18 Coulombs for heat-treated samples and a staggering 360 Coulombs for untreated samples. Such stark contrasts highlight the superior chloride-ion penetration resistance offered by UHPC formulations incorporating recycled glass powder, positioning them as promising candidates for improving the durability and longevity of concrete structures [40].

In the same line, Jaramillo-Murcia et al. [58] also compared the two recycled glass UHPC formulations with the control one but using just standard curing for the specimens. Their results are represented in Figure 18. Notably, the findings reveal a consistent enhancement in durability across different UHPC mixtures and ages. Initially, discernible differences are observed among the mixtures, particularly at the seven-day mark, attributable to variations in packaging density. The Control mixture exhibited Coulombs values of 1161, 80 and 49 at 7, 28 and 90 days, respectively, while Optimized 1 displayed values of 1211, 488 and 75 for the same time intervals. Optimized 2, on the other hand, showed Coulombs values of 2178, 531 and 90 at 7, 28 and 90 days, respectively. However, as the glass content matures within the mixtures, these disparities diminish due to the activation of its pozzolanic properties. Specifically, at 28 days, the penetration of chloride ions for Control and Optimized 1 dosages is deemed negligible, while that of Optimized 2 dosage is exceptionally low. Remarkably, at 90 days, all blend outcomes demonstrate negligible chloride ion penetration, underscoring the exceptional efficacy of the mineral admixtures. These findings not only corroborate the potential application of the investigated UHPCs in infrastructure elements facing harsh environmental conditions, such as coastal environments but also resonate with previous studies conducted on various UHPC dosages by multiple researchers, including Soliman's research. The remarkable performance exhibited by the mineral admixtures further fortifies their suitability for deployment in demanding construction scenarios [58].

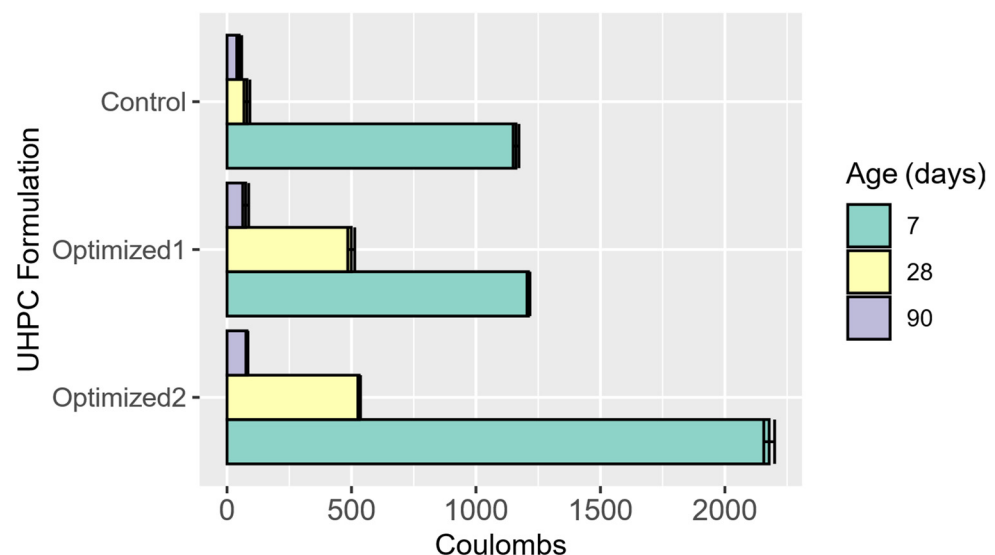


**Figure 18.** Chloride in penetration results of control and optimized UHPC formulations assessed at 7, 18 and 90 days [58].

### 5.5.3. Initial Surface Absorption

The Initial Surface Absorption Test (ISAT) for concrete assesses the rate at which water is absorbed by the concrete's specimen's surface over a specific duration, providing insights into its permeability and potential durability. Figures 19 and 20 present the findings of the ISAT measured during a period of 10 and 30 min respectively, conducted by [12] on the three UHPC dosages depicted in Table 6 and whose particle packing is presented in Figure 6. The data reveal consistently low absorption levels across all samples, with a gradual decline as curing progresses. Notably, there is a marked reduction in absorption values over time for the Control dosage, suggesting potential densification of the structure, likely attributed to pore filling [58,82]. The findings from density, absorption and void testing on hardened concrete support this observation. Figure 19 indicates that the use of recycled glass and limestone powders as a partial cement replacement yields comparable initial absorption rates, as evidenced at the 10-min interval. Similarly, Figure 20 depicts data for the initial absorption rate at 30 min and across all test ages. Analysis indicates a direct

correlation between exposure duration and water absorption, with prolonged exposure resulting in decreased absorption due to surface pore saturation. Further examination reveals the most notable discrepancy between the control dosage and optimized dosages at 7 days of age, with diminishing disparities as curing time progresses. This suggests a gradual convergence in performance as the curing duration extends [58,82].

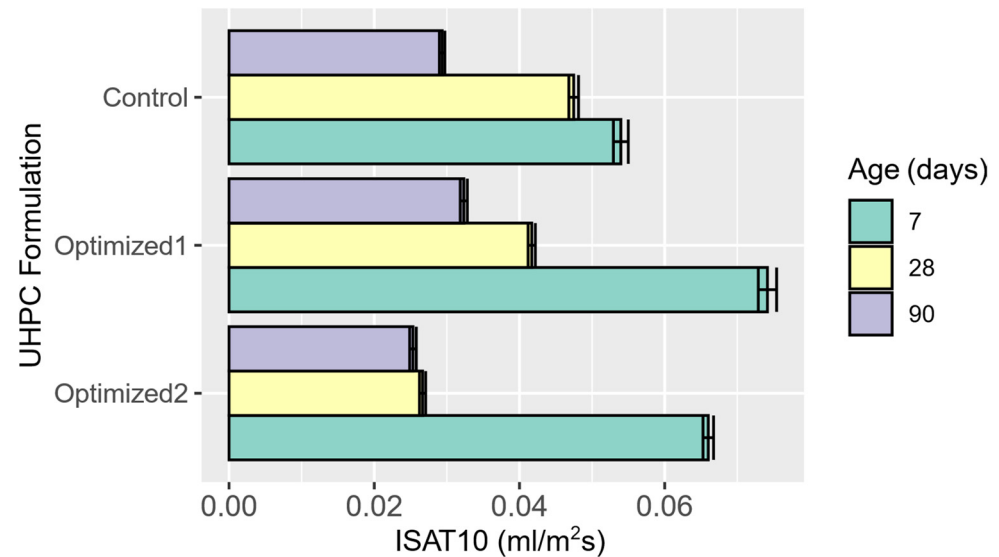


**Figure 19.** ISAT-10 results of control and optimized UHPC formulations assessed at 7, 18 and 90 days [12].

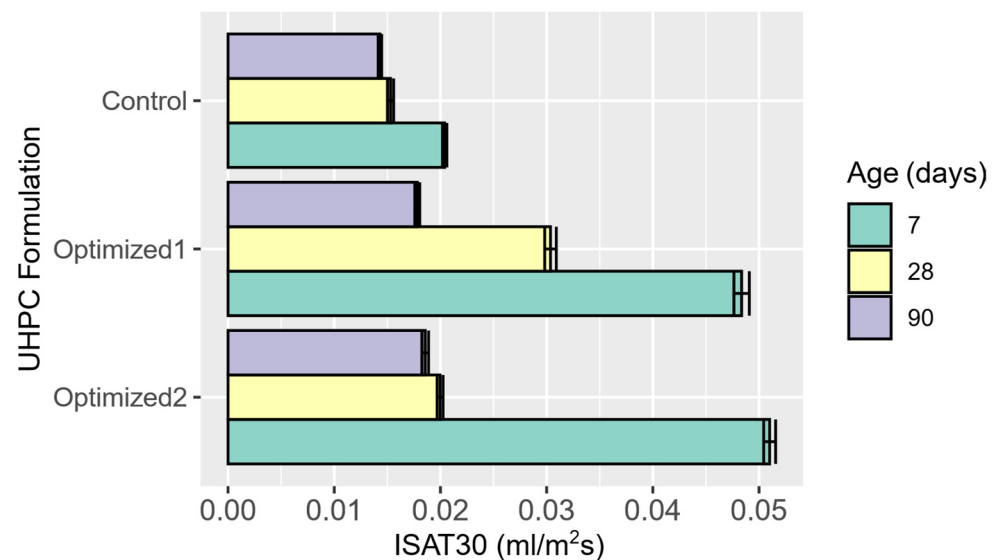


**Figure 20.** ISAT-30 results of control and optimized UHPC formulations assessed at 7, 18 and 90 days [12].

In accordance with the British standard [143], concrete exhibiting absorption rates under  $0.25 \text{ mL/m}^2\text{s}$  for ISAT-10 and  $0.17 \text{ mL/m}^2\text{s}$  for ISAT-30 is defined as low-absorption concrete. As depicted in Figures 19 and 20, the recorded values across all dosages and ages significantly surpass these thresholds. This discrepancy highlights the enhanced microstructure of all UHPC formulations considered [12].

#### 5.5.4. Freeze-Thaw Performance

Freeze-thaw performance represents the ability of a material to withstand the adverse effects of repeated cycles of freezing and thawing. In the context of construction materials,

such as UHPC, resistance to freezing and thawing is a key feature to ensure durability and structural integrity over time, especially in regions with cold climates or subject to extreme seasonal changes [112,144]. A recent study, based on ASTM C 666 specification, evaluated the freeze-thaw resistance of UHPC modified with glass particles [40]. In that research, a portion of the cement was replaced by glass particles in the mixture, resulting in a refined microstructure that enhanced its resistance to the freeze-thaw cycle. During 1000 cycles of freezing and thawing, the recycled glass added UHPC showed no significant signs of deterioration, suggesting excellent freeze-thaw performance [40].

Moreover, the resistance to freeze-thaw cycles, evaluated as per ASTM C666 standard, the aforementioned study put forward a mean dynamic MoE of 101% after 1000 cycles for glass UHPC, with no sign of jeopardizing or cracking at the end of the experiment. In comparison, minimal degradation was observed in traditional UHPC after 600 to 800 cycles, while the relative dynamic modulus decreased to 90% after 1000 freeze-thaw cycles [40].

### 5.5.5. Alkali-Silica Reaction Resistance

When GP is utilized as a cementitious agent, as in the case of glass powder, it does not represent a hazard of ASR expansion in the UHPC, as the pozzolanic action of the glass is activated before the ASR [54,85,145]. The situation could change when recycled glass is used as a substitute for sand, with particle diameters greater than when it is used as cementitious material [91]. In a research conducted by Redondo-Mosquera et al. [49] 100% of the sand was replaced by GS with an average diameter of particles of 300  $\mu\text{m}$  in a UHPC with a w/b less than 0.2. Three mixtures were designed with different amounts of SF (from 100 to 210  $\text{kg}/\text{m}^3$ ) to evaluate the ASR expansion according to ASTM C 1260 [146]. With an amount of 100  $\text{kg}/\text{m}^3$  of SF the volume expansion of the UHPC was 0.28%, which is higher than the 0.1% recommended in ASTM C 1260, however when using 155  $\text{kg}/\text{m}^3$  and 210  $\text{kg}/\text{m}^3$  of SF the results are satisfactory (less than 0.1%). The trend shown in Figure 21 indicated that at such a high glass replacement level it is appropriate to add mineral admixtures with high pozzolanic reactivity to the UHPC in order to mitigate the ASR expansion. The latter is in concordance with what was exposed in [65]. Consistent results were reported for a UHPC with w/cm of 0.189 designed with glass ( $d_{50}$ : 275  $\mu\text{m}$ ) used as a sand replacement. The UHPC volume expansion was no more than 0.05% [69].

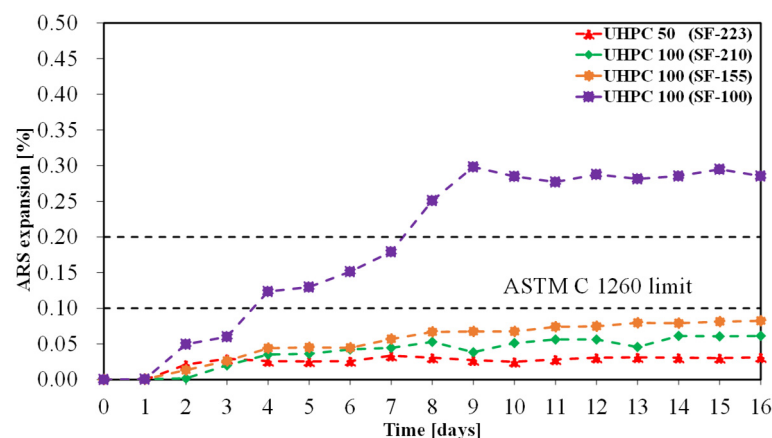


**Figure 21.** Rapid ASR expansion test of UHPC [49,69]. UHPC 50 (SF-223): 50% sand replacement and 223  $\text{kg}/\text{m}^3$  of SF; UHPC 100 (SF-210): 100% sand replacement and 210  $\text{kg}/\text{m}^3$  of SF; UHPC 100 (SF-155): 100% sand replacement and 155  $\text{kg}/\text{m}^3$  of SF; UHPC 100 (SF-100): 100% sand replacement and 100  $\text{kg}/\text{m}^3$  of SF.

### 5.5.6. Resistance to Mechanical Abrasion

Measuring mechanical abrasion resistance is particularly useful for evaluating the durability of materials used in buildings, like concrete, masonry and cementitious products [40,147]. It helps assess how well these materials can withstand abrasive forces encoun-

tered in real-world conditions, such as foot traffic, vehicular traffic and other mechanical actions. Soliman et al. analyzed the influence of GP on UHPC's mechanical abrasion [1,40]. According to the ASTM C944 standard, this resistance is determined by the relative volume loss index [148]. In the case of waste glass–UHPC under study, this index was measured at 1.35 mm after 28 days of standard curing. In comparison, for conventional UHPC, this index varied between 1.1 and 1.7 mm. It is important to note that the maximum specified threshold in ASTM C944 is 3.0 mm [40].

### 5.5.7. Drying Shrinkage

The study presented by [96] delved into the impact of limestone and milled glass powders on UHPC drying shrinkage, by considering the three dosages depicted in Table 6 and Figure 6, with and without fiber reinforcement. As previously stated, three different dosages were examined: two with partial substitution of cement and SF, and one serving as a reference without any substitution [47,59]. By integrating 2% (vol.) of steel microfiber into these three UHPC dosages, fiber-reinforced UHPC samples were successfully produced. Figure 22 depicts the findings of the tests conducted in the aforementioned research. In that figure, 2%Control corresponds to the Control dosage depicted in Table 6 reinforced with 2% of fiber OL 13/0.2, and 2%Optimized 1 and 2%Optimized 2 represented the same fiber reinforcement for Optimized 1 and Optimized 2, respectively. The study demonstrated that the inclusion of limestone and GP enhances the rheological characteristics of concrete, thereby reducing dependence on chemical admixtures and enhancing cost-effectiveness. Thereby, as per this study's findings, partial substitution of cement and SF had been found to effectively mitigate drying shrinkage in both UHPC and UHPFRC compared to Control dosage [96]. The reported experimentation also revealed that incorporating microfibers into reinforcement and adjusting cement and SF proportions significantly reduced UHPC drying shrinkage by up to 40% compared to the Control UHPC formulation. The addition of 2% straight steel fibers led to notable reductions in Control dosage shrinkage, with reductions of 10.8%, 18.1%, 12.1% and 12.2% observed at 5, 15, 20 and 25 days, respectively [96].

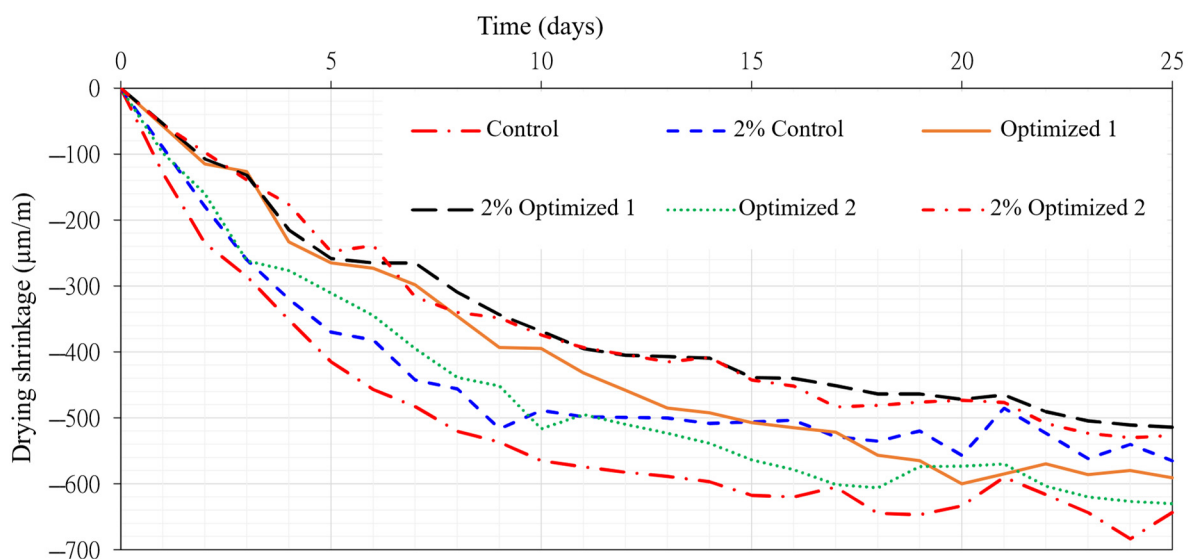


**Figure 22.** Reported drying shrinkage of UHPC formulations depicted in Table 6 with and without 2% volume fiber reinforcement [96].

Significantly, findings also depicted that the incorporation of a substantial volume of fibers into the mix of limestone and GP powders (i.e., into Optimized 1 or Optimized 2) resulted in considerable shrinkage reductions of 40.4%, 28.3%, 25.0% and 18.1% at the same ages [96]. Similar results in the same orders of magnitude were reported by PP when analyzing mixtures with and without UHPC fibers with recycled glass and calcium carbonate. Similar results in the same orders of magnitude were reported

by [12,47,59] when analyzing mixtures with and without UHPC fibers with recycled glass and calcium carbonate.

#### 5.5.8. Resistance to Deicing Salt Scaling

The resistance to deicing salt scaling is a critical factor for assessing concrete durability, especially in structures subjected to saltwater or in which de-icing salts are used, like pavements and bridge decks. In the study conducted by [1,40], this resistance was evaluated on a UHPC mixture proportion that utilized recycled glass powder for total substitution of quartz powder. The UHPC formulation is put forward in Table 10.

**Table 10.** Glass UHPC formulation reported by [40] in kg/m<sup>3</sup>.

Cement	SF	Glass Powder	Quartz Sand	PVA Fiber	Water
549	204	403	888	32.5	224

The test was conducted by measuring mass loss on the concrete surface after 56 freeze-thaw cycles, resulting in a scaled mass of approximately 12 g/m<sup>2</sup>, which compares favorably with the ASTM C672 specified limit of 1000 g/m<sup>2</sup>. This measured value falls within the range reported in the literature for traditional UHPC, which varies from 8 to 60 g/m<sup>2</sup> after 28 to 50 freeze-thaw cycles. As per the authors, these results suggested excellent durability of the concrete evaluated in this study under freeze-thaw cycle exposure conditions, which is promising for its application in structures exposed to marine environments or subject to de-icing salt usage [1,40].

## 6. Impact of Recycled Glass Inclusion on the Life Cycle Assessment of UHPC

Life Cycle Assessment (LCA) is a pivotal methodology employed to comprehensively assess the environmental impact of a product, material or technology by considering its entire life cycle—from raw material extraction to manufacturing, application and disposal. When it comes to UHPC incorporating alternative mineral admixtures, such as recycled glass, LCA serves as a robust tool to quantify and analyze the environmental implications of this innovative construction material [41,52,94]. The LCA analysis considers various stages in the life cycle of UHPC, including the extraction and transportation of raw materials, the manufacturing process, construction and end-of-life scenarios. This holistic approach allows researchers and practitioners to assess the overall environmental footprint, providing insights into potential environmental benefits and areas for improvement [94]. Key aspects taken into account during the LCA analysis include [41,52,94]:

1. **Raw Material Extraction and Transportation:** Examining the environmental impact associated with the extraction of raw materials such as cement, recycled glass and other supplementary materials, as well as the energy-intensive transportation of these materials to the production site.
2. **Manufacturing Process:** Assessing the environmental consequences of the UHPC production process, including energy consumption, emissions and waste generation. This stage is critical for understanding the influence of incorporating recycled glass on factors like carbon footprint and energy efficiency.
3. **Construction Phase:** Considering the environmental impact during the construction phase, which includes transportation of UHPC to the construction site, energy use during placement and potential implications for construction-related activities.
4. **Service Life:** Evaluating the durability and performance of UHPC over its service life, as these factors can significantly influence the overall environmental sustainability of the material.
5. **End-of-Life Scenarios:** Investigating the environmental implications of various end-of-life scenarios, such as recycling, reuse or disposal in landfills. This aspect is particularly relevant for assessing the potential environmental benefits of recycling glass in UHPC compared to conventional end-of-life options.

Therefore, the LCA analysis provides a quantitative and systematic approach to understanding the environmental trade-offs associated with UHPC incorporating recycled glass. By considering these various stages in the life cycle, researchers can identify opportunities for optimization and innovation, ultimately contributing to the development of more sustainable construction materials and practices [41,52,94]. In this sense, a comprehensive study conducted by Tagnit-Hamou et al. [52] demonstrated the noteworthy environmental benefits of incorporating recycled glass into concrete, including those of normal, high and ultra-high strength, compared to conventional end-of-life scenarios such as landfilling. In addition, Abellan-García and colleagues have analyzed the carbon footprint of UHPC dosages which incorporates other mineral admixtures such as LP and RHA in addition to glass powder [47,59,94].

Figure 23 synthesizes the findings from various research works that analyzed the use of alternative mineral admixtures for lowering the carbon footprint of the cement-based material, focusing on the use of waste glass, along with several typical UHPC dosages with higher dosages of cement in their composition. This way, Figure 23 presents a comprehensive view of UHPC dosages, showcasing their coordinates of compressive strength in MPa and their corresponding CO<sub>2</sub>-equivalent emissions. Notably, the increase in CS of analyzed UHPCs corresponded to higher embedded CO<sub>2</sub> emissions and environmental impact. However, as Figure 23 depicts, the compressive strength reached by the UHPC which utilizes waste glass in their composition as alternative SCM outperforms the compressive strength of those with other alternative mineral admixtures, such as LP, GGBFS and FA, for the same range of embedded CO<sub>2</sub> emissions. The reason behind the latter has been reported to lie in the optimized particle-packing model, coupled with cement replacement by waste glass, which emerged as a strategic approach to achieve both ‘greener’ concrete and higher mechanical properties [24,52,63,117]. This design strategy not only reduces CO<sub>2</sub> emissions but also facilitates the reuse of glass, minimizing the need for landfilling and conserving natural resources [50].

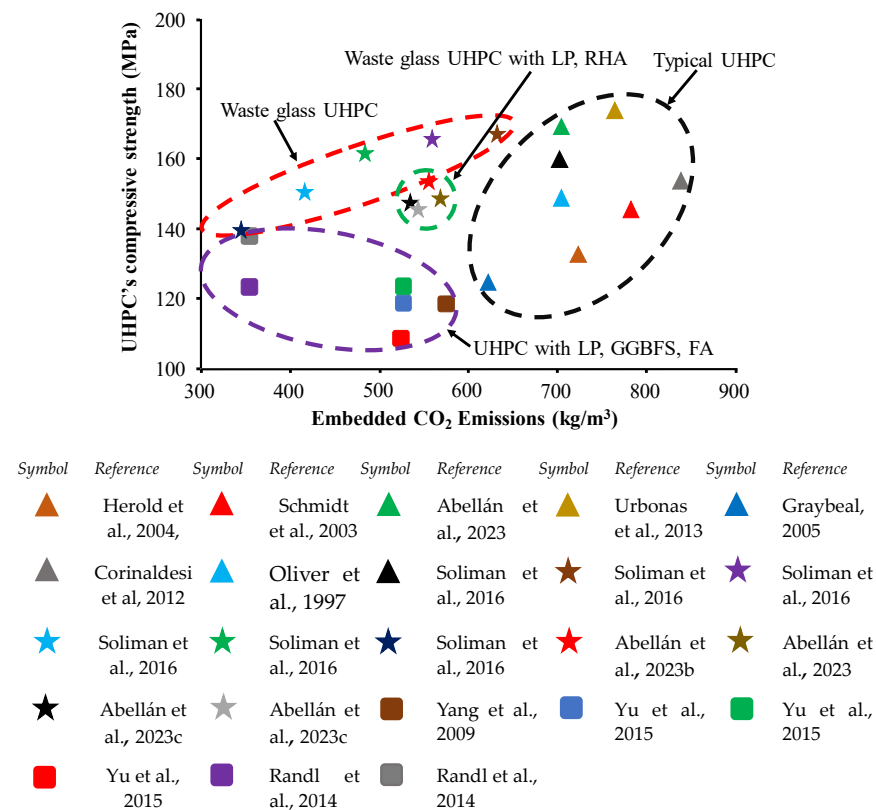


**Figure 23.** Correlation between the amount of embedded CO<sub>2</sub> emissions in kg/m<sup>3</sup> and the UHPC’s CS in MPa for different formulations [41,47,59,94,130,149–156].

## 7. Cost Implications

Over the past decade, considerable data have been acquired on UHPC developments and uses, which has demonstrated that despite its superior qualities, the higher production cost of UHPC—largely due to increased cement, quartz powder and silica fume requirements—is among the causes that have limited its widespread adoption in the construction sector [157]. Therefore, substituting typical UHPC-making ingredients, such as QP, SF, cement and even quartz sand, with ground waste glass has the potential to substantially reduce the expenses associated with traditional UHPC formulations [76,77]. In addition, due to the chemical features depicted in Table 3, the low water absorption (see Table 4) and the lack of porosity of milled waste glass particles, the utilization of GP and GS allows for reducing the necessary amount of HRWR [47,59,82], which has a significant positive impact on the final cost of UHPC [12]. Moreover, the utilization of locally available WG for UHPC manufacturing has the added advantage of reducing material transportation expenses [41].

To illustrate, as per studies conducted in Canada by [41] the cost of quartz powder exceeds that of GP by threefold. For its part, research carried out in Colombia by [12] found that the cost of recycled glass powder after the milling process was about half the price of cement and a tenth of the price of quartz powder. For its part, the cost of glass sand was also reported to be half of that of UHPC typical quartz sand [50]. Moreover, as per [12], the utilization of waste glass and limestone powders as alternative mineral admixtures in Optimized 1 and 2 UHPC formulations (see Table 6) represents a decrease in the final price of about 40% with respect to the Control dosage.

Furthermore, beyond the direct cost savings, incorporating waste glass into UHPC has several indirect economic benefits. For instance, the reduction in cement and silica fume content not only lowers material costs but also reduces mixing times [12,47,59,82], thereby decreasing the overall cost of mixing in plant-recycled-glass-UHPC compared to typical UHPC formulations. This efficiency can further drive down production costs [157].

For its part, the high processing costs, as well as the energy implications of UHPC, are partly due to the extensive use of cement, which functions as an expensive filler [157]. A more effective method of enhancing strength involves improving binder phase packing using cement substitute materials and fine fillers, rather than simply increasing cement content. Recent methodologies for designing economical and efficient UHPC binders incorporate recycled glass achieving high microstructural packing and desirable rheology for flowable concrete, which could lessen the pouring process and formwork costs [47,75,157].

In any case, practical applications of UHPC reveal that its higher initial costs can be offset by savings in construction supplies, labor, transportation expenses and reduced use of lifting and moving equipment on construction sites. The smaller quantity of concrete required, reduced reinforcement, less formwork and improved floor space utilization due to thinner sections all contribute to lowering overall costs [41,157]. In this sense, the properties both in the fresh state, as well as mechanical and durability reported in the present review study, as well as the real case study in Section 8 of this document, support the idea that waste glass-UHPC follows the trend described above. This way, the reduction in material costs depicted before can make UHPC more competitive compared to conventional concretes, potentially expanding its market reach. Moreover, the environmental benefits of using recycled materials such as waste glass could be a hook for attracting projects with sustainability goals and enhancing the marketability of UHPC products.

## 8. Case Study of a Field Application

The waste glass-UHPC has not only remained in laboratory tests. In addition, real-field applications have been reported. Among them, the construction of two similar footbridges, replacing the University of Sherbrooke campus's damaged wooden structures, stands out. The bridge utilized the recycled glass UHPC formulation depicted in Table 10, which was manufactured in the University of Sherbrooke's laboratory [40]. More information about the waste glass-UHPC formulation and mixing procedure can be found in the references [1,40,52].

As per reference [40], the construction of the two pedestrian bridges met the university's architectural and structural requirements for pedestrian applications, as well as aligned with its sustainability policy. The waste glass–UHPC's mechanical properties facilitated the creation of spans with minimal cross-sections, with each bridge weighing approximately four tons. In addition, the concrete exhibited remarkable workability and rheological properties [1]. This may be attributed to GP's particles' completely non-absorbent nature and the meticulously optimized packing density across the concrete matrix [75]. Moreover, the extensive investigation of this material boasted robustness, exceptional abrasion and impact resistance [1,40,52]. The bridge exhibits the following properties: the arch slab has a length of 4.91 m, a width of 2.5 m and a thickness of 0.075 m. It is supported by longitudinal ribs of different heights and a uniform width of 0.13 m [1]. The mid-height of the arch slab was reinforced with welded-wire reinforcement (M10 at 300 mm in both directions), and the bottom of each rib was strengthened with a single M20 reinforcing bar [1].

## 9. Conclusions

After a careful and deep review of 157 documents from the scientific literature, this paper discusses the advantages and disadvantages of using milled WG in the form of GP and/or GS in the manufacture of UHPC mixes, based on past and present research. The following conclusions are drawn:

1. **Environmental and Economic Benefits:** Using WG in UHPC helps preserve the environment and reduces costs by substituting traditional materials such as cement, silica fume, quartz powder and quartz sand. Incorporating waste glass and limestone powders in UHPC formulations substantially lowers production costs, with savings of up to 40% compared to traditional formulations.
2. **Supplementary Cementitious Material:** Due to its high silicon oxide content and amorphous nature, GP, when properly milled, effectively acts as a supplementary cementitious material, enhancing the formation of C-S-H and improving UHPC properties.
3. **Enhanced Hydration Kinetics:** The inclusion of GP improves hydration kinetics, reduces heat of hydration and mitigates microcrack formation.
4. **Compressive Strength:** Substituting up to 25% of cement with GP can enhance compressive strength through pozzolanic reactions. However, cement replacement ratios over 30% may reduce it.
5. **Material Efficiency:** The incorporation of GP allows for significant reductions in cement and silica fume content (up to 30% and 50%, respectively), while maintaining critical compressive strength thresholds above 150 MPa and achieving strengths exceeding 200 MPa in some formulations.
6. **Synergistic Effects with Limestone Powder:** The combined use of GP and limestone powder improves rheology, reduces superplasticizer demand and lowers water-to-binder ratios, enhancing both mechanical properties and sustainability.
7. **Early Strength Development:** The utilization of glass and limestone powder, along with FC3R and MK, shows promising advancements in early strength development. Through the synergy between glass and limestone, the negative effect on the rheology of the aluminum silicates in these components can be mitigated.
8. **Fiber-reinforced UHPC mechanical Performance:** Waste glass–UHPC exhibits bending and direct tensile performances comparable to traditional UHPC with similar fiber reinforcement.
9. **Durability:** The inclusion of milled GP in UHPC has been thoroughly analyzed, focusing on properties such as voids in hardened concrete, chloride penetration, initial surface absorption, freeze-thaw performance, alkali-silica reaction resistance, mechanical abrasion resistance, drying shrinkage and resistance to deicing salt scaling. While the addition of GP generally produces favorable results, slightly lower than traditional UHPC without recycled glass, it demonstrates superior performance in specific areas such as freeze-thaw resilience and drying shrinkage.

10. Environmental Impact: Incorporating GP into UHPC formulations offers significant environmental benefits, as evidenced by life cycle analysis studies. Revised studies have shown that UHPC incorporating recycled glass exhibits lower carbon footprints compared to conventional end-of-life scenarios like landfilling, contributing to sustainability in construction. Furthermore, research indicates that UHPC formulations with GP achieve higher compressive strengths at lower CO<sub>2</sub> emissions, in comparison with other supplementary cementitious materials.
11. Scalable Application: The successful use of WG in UHPC for constructing the foot-bridge at the University of Sherbrooke demonstrates its potential for scalable and practical applications.

## 10. Future Research Directions

Further research is essential to explore the long-term performance and durability of UHPC incorporating various types and proportions of waste glass under diverse environmental conditions. Investigating the impact of glass particle size distribution on UHPC properties and the combined effects of waste glass with other supplementary materials could further enhance UHPC's performance and sustainability. Large-scale field applications and pilot projects are necessary to validate laboratory findings and assess practical implications. Expanded life cycle analyses and cost-benefit studies across different scenarios and locations will provide a comprehensive understanding of the benefits. Additionally, innovative recycling techniques and advanced processing methods for waste glass should be explored to improve its quality and performance in UHPC formulations.

**Funding:** This research received no external funding.

**Acknowledgments:** Special thanks go to the Department of Civil and Environmental Engineering at the Universidad del Norte for their invaluable support and assistance throughout the research process. Additionally, the authors also extend their appreciation to the Karl C. Parrish Jr. Library at the same university for their generous assistance in providing access to essential documents for this review article. Their contributions have been instrumental in the completion of this work.

**Conflicts of Interest:** The authors declare no conflict of interest.

## References

1. Tagnit-Hamou, A.; Soliman, N.A.; Omran, A. Green Ultra-High-Performance Glass Concrete. In Proceedings of the International Interactive Symposium on Ultra-High Performance Concrete 2016, Des Moines, IA, USA, 18–20 July 2016.
2. Abellán-García, J. K-Fold Validation Neural Network Approach for Predicting the One-Day Compressive Strength of UHPC. *Adv. Civ. Eng. Mater.* **2021**, *10*, 223–243. [[CrossRef](#)]
3. Abellán-García, J.; Santofimo-Vargas, M.A.; Torres-Castellanos, N. Analysis of Metakaolin as Partial Substitution of Ordinary Portland Cement in Reactive Powder Concrete. *Adv. Civ. Eng. Mater.* **2020**, *9*, 368–386. [[CrossRef](#)]
4. Nehdi, M.; Abbas, S.; Soliman, A. Exploratory Study of Ultra-High Performance Fiber Reinforced Concrete Tunnel Lining Segments with Varying Steel Fiber Lengths and Dosages. *Eng. Struct.* **2015**, *101*, 733–742. [[CrossRef](#)]
5. *ACI Committe 239R*; ACI Committe 239 ACI—239 Committee in Ultra-High Performance Concrete. ACI: Toronto, ON, Canada, 2018.
6. Ahmad, S.; Hakeem, I.; Maslehuddin, M. Development of UHPC Mixtures Utilizing Natural and Industrial Waste Materials as Partial Replacements of Silica Fume and Sand. *Eur. J. Environ. Civ. Eng.* **2014**, *2014*, 1106–1126. [[CrossRef](#)] [[PubMed](#)]
7. Habel, K.; Charron, J.-P.; Braike, S.; Hooton, R.D.; Gauvreau, P.; Massicotte, B. Ultra-High Performance Fibre Reinforced Concrete Mix Design in Central Canada. *Can. J. Civ. Eng.* **2008**, *35*, 217–224. [[CrossRef](#)]
8. Abellán-García, J.; Fernández-Gómez, J.A.; Torres-Castellanos, N.; Núñez-López, A.M. Machine Learning Prediction of Flexural Behavior of UHPFRC. In *Fibre Reinforced Concrete: Improvements and Innovations, BEFIB 2020*; Serna, P., Llano-Torre, A., Martí-Vargas, J.R., Navarro-Gregori, J., Eds.; RILEM Bookseries: Valencia, Spain, 2020; Volume 4, pp. 570–583. ISBN 978-3-030-58482-5.
9. Abellán-García, J.; Guzmán-Guzmán, J.S. Random Forest-Based Optimization of UHPFRC under Ductility Requirements for Seismic Retrofitting Applications. *Constr. Build. Mater.* **2021**, *285*, 122869. [[CrossRef](#)]
10. Abellán-García, J.; Fernández-Gómez, J.; Torres-Castellanos, N.; Núñez-López, A. Tensile Behavior of Normal Strength Steel Fiber Green UHPFRC. *ACI Mater. J.* **2021**, *118*, 127–138. [[CrossRef](#)]
11. Abellán-García, J.; Guzmán-Guzmán, J.S.; Sánchez-Díaz, J.A.; Rojas-Grillo, J. Experimental Validation of Artificial Intelligence Model for the Energy Absorption Capacity of UHPFRC. *Dyna* **2021**, *88*, 150–159. [[CrossRef](#)]
12. Abellán-García, J. *Dosage Optimization and Seismic Retrofitting Applications of Ultra-High-Performance Fiber Reinforced Concrete (UHPFRC)*; Polytechnic University of Madrid: Madrid, Spain, 2020.

13. Abellán-García, J.; Ortega-Guzmán, J.J.; Chaparro-Ruiz, D.A.; García-Castaño, E. A Comparative Study of LASSO and ANN Regressions for the Prediction of the Direct Tensile Behavior of UHPFRC. *Adv. Civ. Eng. Mater.* **2022**, *11*, 235–262. [[CrossRef](#)]
14. Shi, C.; Wu, Z.; Xiao, J.; Wang, D.; Huang, Z.; Fang, Z. A Review on Ultra High Performance Concrete: Part I. *Raw Materials and Mixture Design. Constr. Build. Mater.* **2015**, *101*, 741–751. [[CrossRef](#)]
15. Neira-Medina, A.; Abellan-Garcia, J.; Torres-Castellanos, N. Flexural Behavior of Environmentally Friendly Ultra-High-Performance Concrete with Locally Available Low-Cost Synthetic Fibers. *Eur. J. Environ. Civ. Eng.* **2021**, *26*, 6281–6304. [[CrossRef](#)]
16. Lowke, D.; Stengel, T.; Schießl, P.; Gehlen, C. Control of Rheology, Strength and Fibre Bond of UHPC with Additions—Effect of Packing Density and Addition Type. In Proceedings of the 3rd International Symposium on UHPC and Nanotechnology for High Performance Construction Materials, Kassel, Germany, 7–9 March 2012; University of Kassel: Kassel, Germany, 2012; pp. 215–224, ISBN 9783862192649.
17. Nguyen, N.-H.; Abellán-García, J.; Lee, S.; Garcia-Castano, E.; Vo, T.P. Efficient Estimating Compressive Strength of Ultra-High Performance Concrete Using XGBoost Model. *J. Build. Eng.* **2022**, *52*, 104302. [[CrossRef](#)]
18. Abellán-García, J.; Sánchez-Díaz, J.; Ospina-Becerra, V. Neural Network-Based Optimization of Fibers for Seismic Retrofitting Applications of UHPFRC. *Eur. J. Environ. Civ. Eng.* **2021**, *26*, 6305–6333. [[CrossRef](#)]
19. de Larrard, F.; Sedran, T.; Larrard, F. Optimization of Ultra-High-Performance Concrete by the Use of a Packing Model. *Cem. Concr. Res.* **1994**, *24*, 997–1009. [[CrossRef](#)]
20. Aghdasi, P.; Heid, A.E.; Chao, S.H. Developing Ultra-High-Performance Fiber-Reinforced Concrete for Large-Scale Structural Applications. *ACI Mater. J.* **2016**, *113*, 559–569. [[CrossRef](#)]
21. Shi, C.; Wu, Z.; Xiao, J.; Wang, D.; Huang, Z.; Fang, Z. A Review on Ultra High Performance Concrete: Part II. Hydration, Microstructure and Properties. *Constr. Build. Mater.* **2015**, *96*, 368–377. [[CrossRef](#)]
22. Wang, D.; Shi, C.; Wu, Z.; Xiao, J.; Huang, Z.; Fang, Z. Durability of an Ultra High Performance Fiber Reinforced Concrete (UHPFRC) under Progressive Aging. *Cem. Concr. Res.* **2015**, *55*, 1–13. [[CrossRef](#)]
23. Abellán-García, J.; Fernández-Gómez, J.; Torres-Castellanos, N. Properties Prediction of Environmentally Friendly Ultra-High-Performance Concrete Using Artificial Neural Networks. *Eur. J. Environ. Civ. Eng.* **2020**, *26*, 2319–2343. [[CrossRef](#)]
24. Abellán, J.; Fernández, J.; Torres, N.; Núñez, A. Development of Cost-Efficient UHPC with Local Materials in Colombia. In Proceedings of the Hipermat 2020—5th International Symposium on UHPC and Nanotechnology for Construction Materials, Kassel, Germany, 11–13 March 2020; Middendorf, B., Fehling, E., Wetzels, A., Eds.; University of Kassel: Kassel, Germany, 2020; pp. 97–98.
25. Abellán-García, J. Four-Layer Perceptron Approach for Strength Prediction of UHPC. *Constr. Build. Mater.* **2020**, *256*, 119465. [[CrossRef](#)]
26. Aghdasi, P.; Ostertag, C.P. Green Ultra-High Performance Fiber-Reinforced Concrete (G-UHP-FRC). *Constr. Build. Mater.* **2018**, *190*, 246–254. [[CrossRef](#)]
27. Abellán-García, J.; Núñez-López, A.; Torres-Castellanos, N.; Fernández-Gómez, J. Effect of FC3R on the Properties of Ultra-High-Performance Concrete with Recycled Glass. *Dyna* **2019**, *86*, 84–92. [[CrossRef](#)]
28. Abellán-García, J.; Torres-Castellanos, N.; Fernández-Gómez, J.A.; Núñez-López, A.M. Ultra-High-Performance Concrete with Local High Unburned Carbon Fly Ash. *Dyna* **2021**, *88*, 38–47. [[CrossRef](#)]
29. Abellán-García, J.; Núñez-López, A.; Torres-Castellanos, N.; Fernández-Gómez, J. Factorial Design of Reactive Powder Concrete Containing Electric Arc Slag Furnace and Recycled Glass Powder. *Dyna* **2020**, *87*, 42–51. [[CrossRef](#)]
30. Mishra, O.; Singh, S.P. An Overview of Microstructural and Material Properties of Ultra-High-Performance Concrete. *J. Sustain. Cem. Mater.* **2019**, *8*, 97–143. [[CrossRef](#)]
31. Tayeh, B.A.; Abu Bakar, B.H.; Megat Johari, M.A.; Voo, Y.L. Utilization of Ultra-High Performance Fibre Concrete (UHPFC) for Rehabilitation—A Review. *Procedia Eng.* **2013**, *54*, 525–538. [[CrossRef](#)]
32. Kalny, M.; Kvasnicka, V.; Komanec, J. First Practical Applications of UHPC in the Czech Republic. In Proceedings of the Proceedings of Hipermat 2016—4th International Symposium on UHPC and Nanotechnology for Construction Materials, Kassel, Germany, 9–11 March 2016; Fehling, E., Middendorf, B., Thiemicke, J., Eds.; University of Kassel: Kassel, Germany, 2016; pp. 147–148.
33. Abellán, J.; Núñez, A.; Arango, S. Pedestrian Bridge of UNAL in Manizales: A New UHPFRC Application in the Colombian Building Market. In Proceedings of the Hipermat 2020—5th International Symposium on UHPC and Nanotechnology for Construction Materials, Kassel, Germany, 11–13 March 2020; Middendorf, B., Fehling, E., Wetzels, A., Eds.; Kassel University Press: Kassel, Germany, 2020; pp. 43–44.
34. Abellán-García, J. An Overview of the Development and Applications of UHPFRC in Colombia. In *Concrete Plant International Worldwide*; Concrete Technology: Cape Town, South Africa, 2020; pp. 48–52. ISBN 1437-9023.
35. Abellán-García, J.; Nuñez-Lopez, A.; Arango-Campo, S. Pedestrian Bridge over Las Vegas Avenue in Medellín. First Latin American Infrastructure in UHPFRC. In *BEFIB 2020*; Serna, P., Llano-Torre, A., Martí-Vargas, J.R., Navarro-Gregori, J., Eds.; RILEM Bookseries: Valencia, Spain, 2020; pp. 864–872. ISBN 978-3-030-58482-5.
36. Dagenais, M.A.; Massicotte, B.; Boucher-Proulx, G. Seismic Retrofitting of Rectangular Bridge Piers with Deficient Lap Splices Using Ultrahigh-Performance Fiber-Reinforced Concrete. *J. Bridg. Eng.* **2018**, *23*, 04017129. [[CrossRef](#)]

37. Rai, B.; Wille, K. Development and Testing of High/Ultra-High Early Strength Concrete. In Proceedings of the 5th International Symposium on Fracture Mechanics of Concrete and Concrete Structures, Vail, CO, USA, 12–16 April 2004; Middendorf, B., Fehling, E., Wetzel, A., Eds.; University of Kassel: Kassel, Germany, 2020; pp. 7–8.
38. Pham, H.D.; Khuc, T.; Nguyen, T.V.; Cu, H.V.; Le, D.B.; Trinh, T.P. Investigation of Flexural Behavior of a Prestressed Girder for Bridges Using Nonproprietary UHPC. *Adv. Concr. Constr.* **2020**, *10*, 71–79. [[CrossRef](#)]
39. Abellán-García, J. Artificial Neural Network Model for Strength Prediction of Ultra-High-Performance Concrete. *ACI Mater. J.* **2021**, *118*, 3–14. [[CrossRef](#)]
40. Soliman, N.A.; Omran, A.F.; Tagnit-Hamou, A. Laboratory Characterization and Field Application of Novel Ultra-High-Performance Glass Concrete. *ACI Mater. J.* **2016**, *113*, 307–316. [[CrossRef](#)]
41. Soliman, N.A.; Tagnit-Hamou, A. Development of Ultra-High-Performance Concrete Using Glass Powder—Towards Ecofriendly Concrete. *Constr. Build. Mater.* **2016**, *125*, 600–612. [[CrossRef](#)]
42. Šerelis, E.; Vaitkevičius, V.; Kerševičius, V. Mechanical Properties and Microstructural Investigation of Ultra-High Performance Glass Powder Concrete. *J. Sustain. Archit. Civ. Eng.* **2016**, *1*, 5–11. [[CrossRef](#)]
43. Shi, C.; Wu, Y.; Riefler, C.; Wang, H. Characteristics and Pozzolanic Reactivity of Glass Powders. *Cem. Concr. Res.* **2005**, *35*, 987–993. [[CrossRef](#)]
44. Hamada, H.; Alattar, A.; Tayeh, B.; Yahaya, F.; Thomas, B. Effect of Recycled Waste Glass on the Properties of High-Performance Concrete: A Critical Review. *Case Stud. Constr. Mater.* **2022**, *17*, e01149. [[CrossRef](#)]
45. Rashad, A.M. Recycled Waste Glass as Fine Aggregate Replacement in Cementitious Materials Based on Portland Cement. *Constr. Build. Mater.* **2014**, *72*, 340–357. [[CrossRef](#)]
46. Rajabipour, F.; Maraghechi, H.; Fischer, G. Investigating the Alkali-Silica Reaction of Recycled Glass Aggregates in Concrete Materials. *J. Mater. Civ. Eng.* **2010**, *22*, 1201–1208. [[CrossRef](#)]
47. Abellan-Garcia, J.; Molinares, M.; Daza, N.; Abbas, Y.M.; Iqbal Khan, M. Formulation of Inexpensive and Green Reactive Powder Concrete by Using Milled-Waste-Glass and Micro Calcium-Carbonate—A Multi-Criteria Optimization Approach. *Constr. Build. Mater.* **2023**, *409*, 134167. [[CrossRef](#)]
48. Kou, S.C.; Xing, F. The Effect of Recycled Glass Powder and Rejected Fly Ash on the Mechanical Properties of Fibre-Reinforced Ultrahigh Performance Concrete. *Hindawi Publ. Corp. Adv. Mater. Sci. Eng.* **2012**, *2012*, 1–8. [[CrossRef](#)]
49. Redondo-Mosquera, J.D.; Sánchez-Angarita, D.; Redondo-Pérez, M.; Gómez-Espitia, J.C.; Abellán-García, J. Development of High-Volume Recycled Glass Ultra-High-Performance Concrete with High C3A Cement. *Case Stud. Constr. Mater.* **2023**, *18*, e01906. [[CrossRef](#)]
50. Abellan-Garcia, J.; Mosquera-Redondo, J.; Khan, M.I.; Abbas, Y.M.; Castro, A. Development of a Novel 124 MPa Strength Green Reactive Powder Concrete Employing Waste Glass and Locally Available Cement. *Arch. Civ. Mech. Eng.* **2023**, *7*, 1–17. [[CrossRef](#)]
51. Du, H.; Tan, K.H. Waste Glass Powder as Cement Replacement in Concrete. *J. Adv. Concr. Technol.* **2014**, *12*, 468–477. [[CrossRef](#)]
52. Tagnit-Hamou, A.; Zidol, A.; Soliman, N.; Deschamps, J.; Omran, A. Ground Glass Pozzolan in Conventional, High, and Ultra-High Performance Concrete. In Proceedings of the 2nd International Congress on Materials & Structural Stability (CMSS-2017), Rabat, Morocco, 22–25 November 2017.
53. Amin, M.; Zeyad, A.M.; Tayeh, B.A.; Agwa, I.S. Effect of Glass Powder on High-Strength Self-Compacting Concrete Durability. *Key Eng. Mater.* **2023**, *495*, 117–127. [[CrossRef](#)]
54. Dhir, R.K.; Dyer, T.D.; Tang, M.C. Alkali-Silica Reaction in Concrete Containing Glass. *Mater. Struct. Constr.* **2009**, *42*, 1451–1462. [[CrossRef](#)]
55. Shaaban, M.; Ahmed, S. Development of Ultra-High Performance Concrete Jointed Precast Decks and Concrete Piles in Integral Abutment Bridges. In Proceedings of the The First International Symposium on Jointless & Sustainable Bridges, Fuzhou, China, 20–22 November 2016.
56. Amin, M.; Agwa, I.S.; Mashaan, N.; Mahmood, S.; Abd-Elrahman, M.H. Investigation of the Physical Mechanical Properties and Durability of Sustainable Ultra-High Performance Concrete with Recycled Waste Glass. *Sustainability* **2023**, *15*, 3085. [[CrossRef](#)]
57. Xu, J.; Zhan, P.; Zhou, W.; Zuo, J.; Shah, S.P.; He, Z. Design and Assessment of Eco-Friendly Ultra-High Performance Concrete with Steel Slag Powder and Recycled Glass Powder. *Powder Technol.* **2023**, *419*, 118356. [[CrossRef](#)]
58. Jaramillo-Murcia, D.C.; Abellán-García, J.; Torres-Castellanos, N.; García-Castaño, E. Properties Analysis of UHPC with Recycled Glass and Limestone Powders. *ACI Mater. J.* **2022**, *119*, 153–164. [[CrossRef](#)]
59. Abellán-García, J.; Daza, N.; Molinares, M.; Abbas, Y.M.; Khan, M.I. Multi-Criteria Optimization of Cost-Effective and Environmentally Friendly Reactive Powder Concrete Incorporating Waste Glass and Micro Calcium Carbonate. *Materials* **2023**, *16*, 6434. [[CrossRef](#)]
60. Wang, H.Y. A Study of the Effects of LCD Glass Sand on the Properties of Concrete. *Waste Manag.* **2009**, *29*, 335–341. [[CrossRef](#)] [[PubMed](#)]
61. Shi, C.; Zheng, K. A Review on the Use of Waste Glasses in the Production of Cement and Concrete. *Resour. Conserv. Recycl.* **2007**, *52*, 234–247. [[CrossRef](#)]
62. Esmaeili, J.; Oudah Al-Mwanes, A. A Review: Properties of Eco-Friendly Ultra-High-Performance Concrete Incorporated with Waste Glass as a Partial Replacement for Cement. *Mater. Today Proc.* **2021**, *42*, 1958–1965. [[CrossRef](#)]
63. Soliman, N.A.; Tagnit-Hamou, A. Using Particle Packing and Statistical Approach to Optimize Eco-Efficient Ultra-High-Performance Concrete. *ACI Mater. J.* **2017**, *114*, 847–858. [[CrossRef](#)]

64. Vaitkevicius, V.; Šerelis, E.; Hilbig, H. The Effect of Glass Powder on the Microstructure of Ultra High Performance Concrete. *Constr. Build. Mater.* **2014**, *68*, 102–109. [CrossRef]
65. Guo, P.; Meng, W.; Nassif, H.; Gou, H.; Bao, Y. New Perspectives on Recycling Waste Glass in Manufacturing Concrete for Sustainable Civil Infrastructure. *Constr. Build. Mater.* **2020**, *257*, 119579. [CrossRef]
66. Siddique, R. Waste Glass. In *Waste Materials and By-Products in Concrete*; Springer: Berlin/Heidelberg, Germany, 2008; pp. 147–175. ISBN 978-3-540-74294-4.
67. Villanueva, A.; Eder, P. *End-of-Waste Criteria for Waste Paper: Technical Proposals*; European Commission: Luxembourg, 2011.
68. Weihua Jin and Stephen Baxter, C.M. “Glascrete”—Concrete with Glass Aggregate. *ACI Mater. J.* **2000**, *97*, 208–213. [CrossRef]
69. Soliman, N.A.; Tagnit-Hamou, A. Using Glass Sand as an Alternative for Quartz Sand in UHPC. *ACI Mater. J.* **2017**, *145*, 847–858. [CrossRef]
70. FEVE. Container Glass Recycling Un Europe. Available online: [https://feve.org/glass\\_recycling\\_stats\\_2018/](https://feve.org/glass_recycling_stats_2018/) (accessed on 1 August 2023).
71. United States Environmental Protection Agency. *Advancing Sustainable Materials Management, 2017 Fact Sheet*; United States Environmental Protection Agency: Washington, DC, USA, 2017.
72. Jiao, Y.; Zhang, Y.; Guo, M.; Zhang, L.; Ning, H.; Liu, S. Mechanical and Fracture Properties of Ultra-High Performance Concrete (UHPC) Containing Waste Glass Sand as Partial Replacement Material. *J. Clean. Prod.* **2020**, *277*, 123501. [CrossRef]
73. Sood, T.; Gurmu, A. Reusing and Repurposing of Glass Waste: A Literature Review. In Proceedings of the 10th World Construction Symposium, Colombo, Sri Lanka, 24–26 June 2022.
74. Al-Awabdeh, F.W.; Al-Kheetan, M.J.; Jweihan, Y.S.; Al-Hamaiedeh, H.; Ghaffar, S.H. Comprehensive Investigation of Recycled Waste Glass in Concrete Using Silane Treatment for Performance Improvement. *Results Eng.* **2022**, *16*, 100790. [CrossRef]
75. Abellán, J.; Fernández, J.; Torres, N.; Núñez, A. Statistical Optimization of Ultra-High-Performance Glass Concrete. *ACI Mater. J.* **2020**, *117*, 243–254. [CrossRef]
76. Esmaeili, J.; AL-Mwanes, A.O. Performance Evaluation of Eco-Friendly Ultra-High-Performance Concrete Incorporated with Waste Glass-A Review. *IOP Conf. Ser. Mater. Sci. Eng.* **2021**, *1094*, 012030. [CrossRef]
77. Soliman, N.A.; Tagnit-Hamou, A. Partial Substitution of Silica Fume with Fine Glass Powder in UHPC: Filling the Micro Gap. *Constr. Build. Mater.* **2017**, *139*, 374–383. [CrossRef]
78. Jain, K.L.; Sancheti, G.; Gupta, L.K. Durability Performance of Waste Granite and Glass Powder Added Concrete. *Constr. Build. Mater.* **2020**, *252*, 119075. [CrossRef]
79. Taha, B.; Nounu, G. Using Lithium Nitrate and Pozzolanic Glass Powder in Concrete as ASR Suppressors. *Cem. Concr. Compos.* **2008**, *30*, 497–505. [CrossRef]
80. Helmy, S.H.; Tahwia, A.M.; Mahdy, M.G.; Elrahman, M.A. Development and Characterization of Sustainable Concrete Incorporating a High Volume of Industrial Waste Materials. *Constr. Build. Mater.* **2023**, *365*, 130160. [CrossRef]
81. Hasan, S.; Nayyef, D. Investigation of Using Waste Glass Powder as a Supplementary Cementitious Material in Reactive Powder Concrete. *Proc. Int. Struct. Eng. Constr.* **2020**, *7*, 1–6. [CrossRef]
82. Abellan-Garcia, J.; Abbas, Y.M.; Khan, M.I.; Pellicer-Martínez, F. ANOVA-Guided Assessment of Waste Glass and Limestone Powder Influence on Ultra-High-Performance Concrete Properties. *Case Stud. Constr. Mater.* **2024**, *20*, e03231. [CrossRef]
83. Abellán-García, J.; García-Castaño, E. Development and Research on Ultra-High-Performance Concrete Dosages in Colombia: A Review. *ACI Mater. J.* **2022**, *119*, 209–221. [CrossRef]
84. Niibori, Y.; Chida, T.; Tochiyama, O. Dissolution Rates of Amorphous Silica in Highly Alkaline Solution. *J. Nucl. Sci. Technol.* **2000**, *37*, 349–357. [CrossRef]
85. Guo, P.; Bao, Y.; Meng, W. Review of Using Glass in High-Performance Fiber-Reinforced Cementitious Composites. *Cem. Concr. Compos.* **2021**, *120*, 104032. [CrossRef]
86. Islam, G.M.S.; Rahman, M.H.; Kazi, N. Waste Glass Powder as Partial Replacement of Cement for Sustainable Concrete Practice. *Int. J. Sustain. Built Environ.* **2017**, *6*, 37–44. [CrossRef]
87. Kunhi Mohamed, A.; Moutzouri, P.; Berruyer, P.; Walder, B.J.; Siramanont, J.; Siramanont, J.; Harris, M.; Negroni, M.; Galmarini, S.C.; Parker, S.C.; et al. The Atomic-Level Structure of Cementitious Calcium Aluminate Silicate Hydrate. *J. Am. Chem. Soc.* **2020**, *142*, 11060–11071. [CrossRef]
88. Kupwade-Patil, K.; Allouche, E.N. Impact of Alkali Silica Reaction on Fly Ash-Based Geopolymer Concrete. *J. Mater. Civ. Eng.* **2013**, *25*, 131–139. [CrossRef]
89. Shayan, A.; Xu, A. Value-Added Utilisation of Waste Glass in Concrete. *Cem. Concr. Res.* **2004**, *34*, 81–89. [CrossRef]
90. Idir, R.; Cyr, M.; Tagnit-Hamou, A. Use of Waste Glass in Cement-Based Materials. In Proceedings of the SBEIDCO—1st International Conference on Sustainable Built Environment Infrastructures in Developing Countries, Orán, Algeria, 12–14 October 2009; pp. 109–116.
91. Kaminsky, A.; Krstic, M.; Rangaraju, P.; Tagnit-Hamou, A.; Thomas, M.D.A. Ground-Glass Pozzolan for Use in Concrete. *Concr. Int.* **2020**, *42*, 24–32.
92. Shao, Y.; Lefort, T.; Moras, S.; Rodriguez, D. Studies on Concrete Containing Ground Waste Glass. *Cem. Concr. Res.* **2000**, *30*, 91–100. [CrossRef]
93. Abellan-Garcia, J. Tensile Behavior of Recycled-Glass-UHPC under Direct Tensile Loading. *Case Stud. Constr. Mater.* **2022**, *17*, 1–16. [CrossRef]

94. Abellan-garcia, J.; Martinez, D.M.; Khan, M.I.; Abbas, Y.M.; Pellicer-martí, F. Environmentally Friendly Use of Rice Husk Ash and Recycled Glass Waste to Produce Ultra-High- Performance Concrete. *J. Mater. Res. Technol.* **2023**, *25*, 1869–1881. [[CrossRef](#)]
95. Abellan-Garcia, J. Effect of Rice Husk Ash as Partial Replacement of Ordinary Portland Cement in Ultra-High-Performance Glass Concrete. *Eur. J. Environ. Civ. Eng.* **2023**, *2*, 396–401. [[CrossRef](#)]
96. Abellan-Garcia, J.; Iqbal Khan, M.; Abbas, Y.M.; Martínez-Lirón, V.; Carvajal-Muñoz, J.S. The Drying Shrinkage Response of Recycled-Waste-Glass-Powder-and Calcium-Carbonate-Based Ultrahigh-Performance Concrete. *Constr. Build. Mater.* **2023**, *379*, 131163. [[CrossRef](#)]
97. Abellán-garcía, J.; Iqbal-khan, M.; Abbas, Y.M.; Pellicer-martínez, F. Predicting the Flowability of UHPC and Identifying Its Significant Influencing Factors Using an Accurate ANN Model. *Dyna* **2024**, *91*, 27–36. [[CrossRef](#)]
98. De Larrard, F. *Concrete Mixture Proportioning: A Scientific Approach*; Modern Concrete Technology Series; CRC Press: Boca Raton, FL, USA, 1999.
99. De Larrard, F.; Sedran, T. Mixture-Proportioning of High-Performance Concrete. *Cem. Concr. Res.* **2002**, *32*, 1699–1704. [[CrossRef](#)]
100. Nguyen, N.H.; Abellán-García, J.; Lee, S.; Nguyen, T.K.; Vo, T.P. Simultaneous Prediction the Strain and Energy Absorption Capacity of Ultra-High Performance Fiber Reinforced Concretes by Using Multi-Output Regression Model. *Constr. Build. Mater.* **2023**, *384*, 131418. [[CrossRef](#)]
101. Abellan-Garcia, J.; Fernández, J.; Khan, M.I.; Abbas, Y.M.; Carrillo, J. Uniaxial Tensile Ductility Behavior of Ultrahigh-Performance Concrete Based on the Mixture Design—Partial Dependence Approach. *Cem. Concr. Compos.* **2023**, *140*, 105060. [[CrossRef](#)]
102. Huang, H.; Gao, X.; Wang, H.; Ye, H. Influence of Rice Husk Ash on Strength and Permeability of Ultra-High Performance Concrete. *Constr. Build. Mater.* **2017**, *149*, 621–628. [[CrossRef](#)]
103. Chindaprasirt, P.; Homwuttitwong, S.; Jaturapitakkul, C. Strength and Water Permeability of Concrete Containing Palm Oil Fuel Ash and Rice Husk-Bark Ash. *Constr. Build. Mater.* **2007**, *21*, 1492–1499. [[CrossRef](#)]
104. Yang, R.; Yu, R.; Shui, Z.; Guo, C.; Wu, S.; Gao, X.; Peng, S. The Physical and Chemical Impact of Manufactured Sand as a Partial Replacement Material in Ultra-High Performance Concrete (UHPC). *Cem. Concr. Compos.* **2019**, *99*, 203–213. [[CrossRef](#)]
105. National Cancer Institute Crystalline Silica. Available online: <https://www.cancer.gov/about-cancer/causes-prevention/risk/substances/crystalline-silica> (accessed on 1 August 2023).
106. Mousa, M.; Cuenca, E.; Ferrara, L.; Roy, N.; Tagnit-Hamou, A. Tensile Characterization of an “Eco-Friendly” UHPFRC with Waste Glass Powder and Glass Sand. In Proceedings of the Strain-Hardening Cement-Based Composites. SHCC 2017, Dresden, Germany, 18–20 September 2017; Mechtcherine, V., Slowik, V., Kabele, P., Eds.; RILEM Bookseries: Valencia, Spain, 2017; pp. 238–248.
107. Azmee, N.M.; Shafiq, N. Ultra-High Performance Concrete: From Fundamental to Applications. *Case Stud. Constr. Mater.* **2018**, *9*, e00197. [[CrossRef](#)]
108. Pedrajas, C.; Rahhal, V.; Talero, R. Determination of Characteristic Rheological Parameters in Portland Cement Pastes. *Constr. Build. Mater.* **2014**, *51*, 484–491. [[CrossRef](#)]
109. Mirzahosseini, M.; Riding, K.A. Effect of Curing Temperature and Glass Type on the Pozzolanic Reactivity of Glass Powder. *Cem. Concr. Res.* **2014**, *58*, 103–111. [[CrossRef](#)]
110. Jansen, D.; Neubauer, J.; Goetz-Neunhoeffler, F.; Haerzschel, R.; Hergeth, W.D. Change in Reaction Kinetics of a Portland Cement Caused by a Superplasticizer—Calculation of Heat Flow Curves from XRD Data. *Cem. Concr. Res.* **2012**, *42*, 327–332. [[CrossRef](#)]
111. Li, W.; Huang, Z.; Zu, T.; Shi, C.; Duan, W.H.; Shah, S.P. Influence of Nanolimestone on the Hydration, Mechanical Strength, and Autogenous Shrinkage of Ultrahigh-Performance Concrete. *J. Mater. Civ. Eng.* **2016**, *28*, 1–9. [[CrossRef](#)]
112. Li, J.; Wu, Z.; Shi, C.; Yuan, Q.; Zhang, Z. Durability of Ultra-High Performance Concrete—A Review. *Constr. Build. Mater.* **2020**, *255*, 119296. [[CrossRef](#)]
113. Lee, N.K.; Koh, K.T.; Park, S.H.; Ryu, G.S. Microstructural Investigation of Calcium Aluminate Cement-Based Ultra-High Performance Concrete (UHPC) Exposed to High Temperatures. *Cem. Concr. Res.* **2017**, *102*, 109–118. [[CrossRef](#)]
114. Ge, W.; Zhang, Z.; Ashour, A.; Li, W.; Jiang, H.; Hu, Y.; Shuai, H.; Sun, C.; Li, S.; Liu, Y.; et al. Hydration Characteristics, Hydration Products and Microstructure of Reactive Powder Concrete. *J. Build. Eng.* **2023**, *69*, 106306. [[CrossRef](#)]
115. Amin, M.; Zeyad, A.M.; Tayeh, B.A.; Saad Agwa, I. Effects of Nano Cotton Stalk and Palm Leaf Ashes on Ultrahigh-Performance Concrete Properties Incorporating Recycled Concrete Aggregates. *Constr. Build. Mater.* **2021**, *302*, 124196. [[CrossRef](#)]
116. Bahmani, H.; Mostofinejad, D. Microstructure of Ultra-High-Performance Concrete (UHPC)—A Review Study. *J. Build. Eng.* **2022**, *50*, 104118. [[CrossRef](#)]
117. Fariied, A.S.; Mostafa, S.A.; Tayeh, B.A.; Tawfik, T.A. Mechanical and Durability Properties of Ultra-High Performance Concrete Incorporated with Various Nano Waste Materials under Different Curing Conditions. *J. Build. Eng.* **2021**, *43*, 102569. [[CrossRef](#)]
118. Cheyrezy, M.; Maret, V.; Frouin, L. Microstructural Analysis of RPC (Reactive Powder Concrete). *Cem. Concr. Res.* **1995**, *25*, 1491–1500. [[CrossRef](#)]
119. Maso, J.C. (Ed.) *Interfacial Transition Zone in Concrete*; CRC Press: Boca Raton, FL, USA, 1996.
120. Reda, M.M.; Shrive, N.G.; Gillott, J.E. Microstructural Investigation of Innovative UHPC. *Cem. Concr. Res.* **1999**, *29*, 323–329. [[CrossRef](#)]
121. Demiss, B.A.; Oyawa, W.O.; Shitote, S.M. Mechanical and Microstructural Properties of Recycled Reactive Powder Concrete Containing Waste Glass Powder and Fly Ash at Standard Curing. *Cogent Eng.* **2018**, *5*, 1464877. [[CrossRef](#)]
122. ACI. *ACI Committe 239R Ultra-High-Performance Concrete: An Emerging Technology Report*; ACI: Toronto, ON, Canada, 2018.

123. Hassan, A.M.T.; Jones, S.W.; Mahmud, G.H. Experimental Test Methods to Determine the Uniaxial Tensile and Compressive Behaviour of Ultra High Performance Fibre Reinforced Concrete (UHPFRC). *Constr. Build. Mater.* **2012**, *37*, 874–882. [[CrossRef](#)]
124. Shafieifar, M.; Farzad, M.; Azizinamini, A. Experimental and Numerical Study on Mechanical Properties of Ultra High Performance Concrete (UHPC). *Constr. Build. Mater.* **2017**, *156*, 402–411. [[CrossRef](#)]
125. Nassif, H.; Najm, H.; Sukawang, N. Effect of Pozzolanic Materials and Curing Methods on the Elastic Modulus of HPC. *Cem. Concr. Compos.* **2005**, *27*, 661–670. [[CrossRef](#)]
126. Yoo, D.Y.; Kim, M.J.; Kim, S.W.; Park, J.J. Development of Cost Effective Ultra-High-Performance Fiber-Reinforced Concrete Using Single and Hybrid Steel Fibers. *Constr. Build. Mater.* **2017**, *150*, 383–394. [[CrossRef](#)]
127. Kim, D.J.; Park, S.H.; Ryu, G.S.; Koh, K.T. Comparative Flexural Behavior of Hybrid Ultra High Performance Fiber Reinforced Concrete with Different Macro Fibers. *Constr. Build. Mater.* **2014**, *25*, 4144–4155. [[CrossRef](#)]
128. Abellán-García, J. Comparison of Artificial Intelligence and Multivariate Regression in Modeling the Flexural Behavior of UHPFRC. *Dyna* **2020**, *87*, 239–248. [[CrossRef](#)]
129. Yu, R.; Spiesz, P.; Brouwers, H.J.H. Mix Design and Properties Assessment of Ultra-High Performance Fibre Reinforced Concrete (UHPFRC). *Cem. Concr. Res.* **2014**, *56*, 29–39. [[CrossRef](#)]
130. Yu, R.; Spiesz, P.; Brouwers, H.J.H. Development of an Eco-Friendly Ultra-High Performance Concrete (UHPC) with Efficient Cement and Mineral Admixtures Uses. *Cem. Concr. Compos.* **2015**, *55*, 383–394. [[CrossRef](#)]
131. Wu, Z.; Shi, C.; He, W.; Wu, L. Effects of Steel Fiber Content and Shape on Mechanical Properties of Ultra High Performance Concrete. *Constr. Build. Mater.* **2016**, *103*, 8–14. [[CrossRef](#)]
132. Monte, R.; Pereira, L.d.S.; Figueiredo, A.D.d.; Blanco, A.; Bitencourt Júnior, L.A.G. Simplified DEWS Test for Steel Fibre-Reinforced Concrete Characterisation. *Rev. IBRACON Estruturas Mater.* **2023**, *16*, e16604. [[CrossRef](#)]
133. Maya Duque, L.F.; Graybeal, B. Fiber Orientation Distribution and Tensile Mechanical Response in UHPFRC. *Mater. Struct. Constr.* **2017**, *50*, 55. [[CrossRef](#)]
134. Wille, K.; Kim, D.; Naaman, A.E. Strain Hardening UHP-FRC with Low Fiber Contents. *Mater. Struct.* **2011**, *44*, 538–598. [[CrossRef](#)]
135. Graybeal, B.A.; Baby, F. Development of Direct Tension Test Method for Ultra-High-Performance Fiber-Reinforced Concrete. *ACI Mater. J.* **2013**, *110*, 177–186. [[CrossRef](#)]
136. Abellán-García, J. Artificial Neural Network-Based Methodology for Optimization of Low-Cost Green UHPFRC Under Ductility Requirements. In *Numerical Modeling Strategies for Sustainable Concrete Structures*; Rossi, P., Tailhan, J.-L., Eds.; Springer: Cham, Switzerland, 2023; pp. 1–11. ISBN 9783031077463.
137. Kim, J.J.; Jang, Y.S.; Yoo, D.Y. Enhancing the Tensile Performance of Ultra-High-Performance Concrete through Novel Curvilinear Steel Fibers. *J. Mater. Res. Technol.* **2020**, *9*, 7570–7582. [[CrossRef](#)]
138. Meng, W.; Khayat, K.H. Effect of Hybrid Fibers on Fresh Properties, Mechanical Properties, and Autogenous Shrinkage of Cost-Effective UHPC. *J. Mater. Civ. Eng.* **2018**, *30*, 04018030. [[CrossRef](#)]
139. Kim, D.J.; Wille, K.; Naaman, A.E.; El-Tawil, S. Strength Dependent Tensile Behavior of Strain Hardening Fiber Reinforced Concrete. In *High Performance Fiber Reinforced Cement Composites 6*; Springer: Berlin/Heidelberg, Germany, 2011; pp. 3–10.
140. Shaikh, F.U.A.; Nishiwaki, T.; Kwon, S. Effect of Fly Ash on Tensile Properties of Ultra-High Performance Fiber Reinforced Cementitious Composites (UHP-FRCC). *J. Sustain. Cem. Mater.* **2018**, *7*, 357–371. [[CrossRef](#)]
141. Ghafari, E.; Costa, H.; Júlio, E.; Portugal, A.; Durães, L. Enhanced Durability of Ultra High Performance Concrete by Incorporating Supplementary Cementitious Materials. In *Proceedings of the Second International Conference Microdurability, Amsterdam, The Netherlands, 11–13 April 2012*; pp. 11–13.
142. Abellán-García, J.; Khan, M.I.; Abbas, Y.M.; Castro-Cabeza, A.; Carrillo, J. Multi-Criterion Optimization of Low-Cost, Self-Compacted and Eco-Friendly Micro-Calcium-Carbonate- and Waste-Glass-Flour-Based Ultrahigh-Performance Concrete. *Constr. Build. Mater.* **2023**, *371*, 130793. [[CrossRef](#)]
143. BS1881-208; Recommendations for the Determination of the Initial Surface Absorption of Concrete. British Standards: London, UK, 1996.
144. Liu, Z.; El-Tawil, S.; Hansen, W.; Wang, F. Effect of Slag Cement on the Properties of Ultra-High Performance Concrete. *Constr. Build. Mater.* **2018**, *190*, 830–837. [[CrossRef](#)]
145. Taha, B.; Nounu, G. Utilizing Waste Recycled Glass as Sand/Cement Replacement in Concrete. *J. Mater. Civ. Eng.* **2009**, *21*, 709–721. [[CrossRef](#)]
146. Graybeal, B.; Tanesi, J. Durability of an Ultrahigh-Performance Concrete. *J. Mater. Civ. Eng.* **2007**, *19*, 848–854. [[CrossRef](#)]
147. Sadek, M.M.; Hassan, A.A.A. Abrasion and Scaling Resistance of Lightweight Self Consolidating Concrete Containing Expanded Slate Aggregate. *ACI Mater. J.* **2021**, *118*, 31–42. [[CrossRef](#)]
148. Adresi, M.; Lacidogna, G. Investigating the Micro/Macro-Texture Performance of Roller-Compacted Concrete Pavement under Simulated Traffic Abrasion. *Appl. Sci.* **2021**, *11*, 5704. [[CrossRef](#)]
149. Bonneau, O.; Lachemi, M.; Dallaire, E.; Dugat, J.; Aitcin, P.C. Mechanical Properties and Durability of Two Industrial Reactive Powder Concretes. *ACI Mater. J.* **1997**, *94*, 286–290. [[CrossRef](#)] [[PubMed](#)]
150. Yang, S.L.; Millard, S.G.; Soutsos, M.N.; Barnet, S.J.; Le, T.T. Influence of Aggregate and Curing Regime on the Mechanical Properties of Ultra-High Performance Fibre Reinforced Concrete (UHPFRC). *Constr. Build. Mater.* **2009**, *23*, 2291–2298. [[CrossRef](#)]

151. Randl, N.; Steiner, T.; Ofner, S.; Baumgartner, E.; Mészöly, T. Development of UHPC Mixtures from an Ecological Point of View. *Constr. Build. Mater.* **2014**, *67*, 373–378. [[CrossRef](#)]
152. Herold, G.; Müller, H.S. Measurement of Porosity of Ultra High Strength Fibre Reinforced Concrete. In Proceedings of the International Symposium on Ultra-High Performance Concrete, Kassel, Germany, 13–15 September 2004; Kassel University Press: Kassel, Germany, 2004; pp. 685–694.
153. Schmidt, M.; Fehling, E.; Teichmann, T.; Kai, B.; Roland, B. Ultra-High Performance Concrete: Perspective for the Precast Concrete Industry. *Betonw. Fert. Precast. Plant Technol.* **2003**, *69*, 16–29.
154. Urbonas, L.; Heinz, D.; Gerlicher, T. Ultra-High Performance Concrete Mixes with Reduced Portland Cement Content. *J. Sustain. Archit. Civ. Eng.* **2013**, *3*, 47–51. [[CrossRef](#)]
155. Graybeal, B.A. *Characterization of the Behaviour of Ultra-High Performance Concrete*; University of Maryland: College Park, MD, USA, 2005.
156. Corinaldesi, V.; Moriconi, G. Mechanical and Thermal Evaluation of Ultra High Performance Fiber Reinforced Concretes for Engineering Applications. *Constr. Build. Mater.* **2012**, *26*, 289–294. [[CrossRef](#)]
157. Akeed, M.H.; Qaidi, S.; Ahmed, H.U.; Faraj, R.H.; Mohammed, A.S.; Emad, W.; Tayeh, B.A.; Azevedo, A.R.G. Ultra-High-Performance Fiber-Reinforced Concrete. Part IV: Durability Properties, Cost Assessment, Applications, and Challenges. *Case Stud. Constr. Mater.* **2022**, *17*, e01271. [[CrossRef](#)]

**Disclaimer/Publisher’s Note:** The statements, opinions and data contained in all publications are solely those of the individual author(s) and contributor(s) and not of MDPI and/or the editor(s). MDPI and/or the editor(s) disclaim responsibility for any injury to people or property resulting from any ideas, methods, instructions or products referred to in the content.